Shear resistance and design of stainless steel plate girders in fire

Merih Kucukler

School of Engineering, University of Warwick, Coventry, CV4 7AL, UK

Abstract

In this paper, the shear resistance and design of stainless steel plate girders at elevated temperatures are investigated. A broad range of parameters influencing the structural response of stainless steel plate girders in fire are taken into account, considering (i) austenitic and duplex stainless steel grades, (ii) rigid and non-rigid end posts, (iii) different aspect ratios for the unstiffened portions of the plate girders, (iv) various web slendernesses and (v) different elevated temperature levels. The influence of these parameters on the behaviour of stainless steel plate girders at elevated temperatures is considered. Currently, there is an absence of specific design rules on the fire design of stainless steel plate girders in the European structural steel fire design standard EN 1993-1-2. Considering this, an accuracy assessment of the room temperature stainless steel plate girder design recommendations of the European structural stainless steel design standard EN 1993-1-4 applied with the elevated temperature material properties of stainless steel is performed. The results indicate that this approach leads to unsafe and scattered ultimate strength estimations for stainless steel plate girders in fire. New fire design recommendations for stainless steel plate girders that are in accordance with the existing design provisions of EN 1993-1-2 and EN 1993-1-4 are proposed. The accuracy and safety of the proposed new design recommendations are comprehensively verified against the results from nonlinear finite element modelling.

Keywords: Fire; stainless steel; finite element modelling; imperfections; local buckling; residual stresses; shear

1. Introduction

Stainless steel plate girders are increasingly utilised in the construction industry such as in bridges, buildings and offshore structures in view of their very high corrosion resistance, excellent durability, favourable mechanical properties and considerably enhanced strength and stiffness retention in fire relative to carbon steel plate girders. Stainless steel plate girders generally carry large transverse loads and typically involve highly slender webs to achieve the efficiency in material use, which make them particularly susceptible to shear buckling. There exist comprehensive previous research into the structural response and design of stainless

Email address: merih.kucukler@warwick.ac.uk (Merih Kucukler)

steel plate girders at room temperature [1–8]. However, the research into the behaviour and design of stainless steel plate girders in fire is very scarce. Moreover, the existing design standards such as the European structural steel fire design standard EN 1993-1-2 [9] does not involve specific fire design methods for stainless steel plate girders. Typically, due to the lack of specific fire design rules, the use of room temperature design rules with the reduced material strength and stiffness at elevated temperatures is adopted for the fire design of stainless steel plate girders. Thus far, the accuracy and safety of this approach have not been extensively assessed though, which highlights the need for comprehensive research into the behaviour and design of stainless steel plate girders in fire.

Previous research on stainless steel plate girders predominantly focused on their room temperature structural response and design. Olsson [1], Estrada et al. [2], Real et al. [3] and Saliba and Gardner [4] performed a series of physical experiments on austenitic and duplex stainless steel plate girders with rigid and non-rigid end posts at room temperature. These studies identified that the improvement of the rotated stress field method of EN 1993-1-4 [10] which is based on the proposals of Höglund [11–13] is necessary to obtain more accurate room temperature ultimate resistance predictions for stainless steel plate girders. On the basis of these observations, Saliba et al. [5] put forward new design equations for the room temperature design of stainless steel plate girders, utilising the data from experiments performed on stainless steel plate girders at room temperature from previous studies [1–4]. Two set of design formulae were put forward in Saliba et al. [5] for the room temperature design of stainless steel plate girders with rigid and non-rigid end posts, which were adopted in the latest version of EN 1993-1-4 [10]. In addition to the aforementioned studies [1–5], [6–8] also carried out experimental and numerical investigations into the room temperature response of stainless steel plate girders. The behaviour of stainless steel columns, beams and beam-columns in fire was also experimentally investigated in the literature. Gardner and Baddoo [14], Uppfelt et al. [15], Tondini et al. [16], Fan et al. [17–19], Ding et al. [20], Liu et al. [21, 22] and Xing et al. [23] carried out fire experiments on stainless steel columns, while Xing et al. [24, 25] and Fan et al. [26, 27] performed physical experiments on stainless steel beams and beam-columns in fire. In Gardner and Baddoo [14], stainless steel beams were also tested in fire. In addition to the experiments on stainless steel elements in fire, He et al. [28–30], Lan et al. [31] also tested stainless steel members following their exposure to fire.

Despite the presence of a high number of research studies into the behaviour of stainless steel plate girders at room temperature and stainless steel columns, beams and beam-columns in fire in the literature, there is very limited research into the elevated temperature behaviour and design of stainless steel plate girders, where Reis et al. [32] assessed the accuracy of adopting the room temperature stainless steel plate girder design rules of EN 1993-1-4 [10] with the elevated temperature material properties of stainless steel for the design of stainless steel plate girders in fire. It was highlighted in [32] that the use of the EN 1993-1-4 [9] room temperature stainless steel plate girder design rules with the elevated temperature material properties of stainless steel can lead to scattered and unsafe ultimate resistance predictions for stainless steel plate girders in fire and new, bespoke fire design rules are necessary for stainless steel plate girders. However, thus far, no new fire design proposals

that are in accordance with EN 1993-1-2 [9] and EN 1993-1-4 [10] have been put forward for the accurate and safe design of stainless steel plate girders at elevated temperatures.

Taking into account the very limited research on the topic in the literature, a comprehensive investigation is performed into the behaviour and design of stainless steel plates in fire in this paper. The investigated topic is of importance in that the fire design of stainless steel plate girders in bridges, buildings and offshore structures have to be performed adequately to avoid catastrophic consequences that may result from their inaccurate fire design in the case of a fire event. The influence of a high number of parameters on the elevated temperature response of stainless steel plate girders is taken into consideration in this study, accounting for (i) austenitic and duplex stainless steel grades, (ii) rigid and non-rigid end posts, (iii) different aspect ratios for the unstiffened portions of the plate girders, (iv) various web slendernesses and (v) different elevated temperature levels. Nonlinear shell finite element models of stainless steel plate girders are created. The accuracy of the developed finite element models in mimicking the behaviour of steel plate girders is verified against physical experiments from the literature. The accuracy of using the room temperature design rules provided in EN 1993-1-4 [10] with the elevated temperature material properties of stainless steel for the design of stainless steel plate girders in fire is investigated, where it is observed that this approach can provide inaccurate and unsafe resistance predictions. New design proposals that are in accordance with the existing rules of EN 1993-1-2 [9] and EN 1993-1-4 [10] are made for the fire design of stainless steel plate girders. High accuracy, safety and reliability of the new fire design proposals are demonstrated using the benchmark structural performance data obtained from nonlinear shell finite element models, considering a broad range of parameters influencing the structural response of stainless steel plate girders in fire.

2. Finite element modelling

The shell finite element models of stainless steel plate girders are created and validated against physical experiments from the literature in this section. Following their validation, the shell finite element models are employed to generate comprehensive structural performance data, considering various parameters that can influence the behaviour of stainless steel plate girders at elevated temperatures. The generated comprehensive structural performance data is utilised in the following sections in the assessment of the accuracy of EN 1993-1-2 [9] and development of new fire design proposals for stainless steel plate girders.

2.1. Development of finite element models

In this study, the finite element analysis software Abaqus [33] was employed to create the finite element models of stainless steel plate girders. The four-noded reduced integration shell element denoted as S4R in the Abaqus finite element library [33] was utilised to create all the finite element models; this element which has been successfully used in previous similar studies [34–36] has the ability to take into account transverse shear deformations and membrane stresses. A high mesh density was adopted, taking the element size equal to 10 mm $\times$ 10 mm for all the considered plate girders which enabled the accurate consideration of local and shear buckling effects as well as the development and spread of plasticity within

the finite element models. Note that a mesh sensitivity analysis was performed in the determination of the adopted mesh size in the development of the finite element models. The loading and boundary conditions of the finite element models of stainless steel plates girders with rigid and non-rigid end posts are illustrated in Fig. 1. As can be seen from the

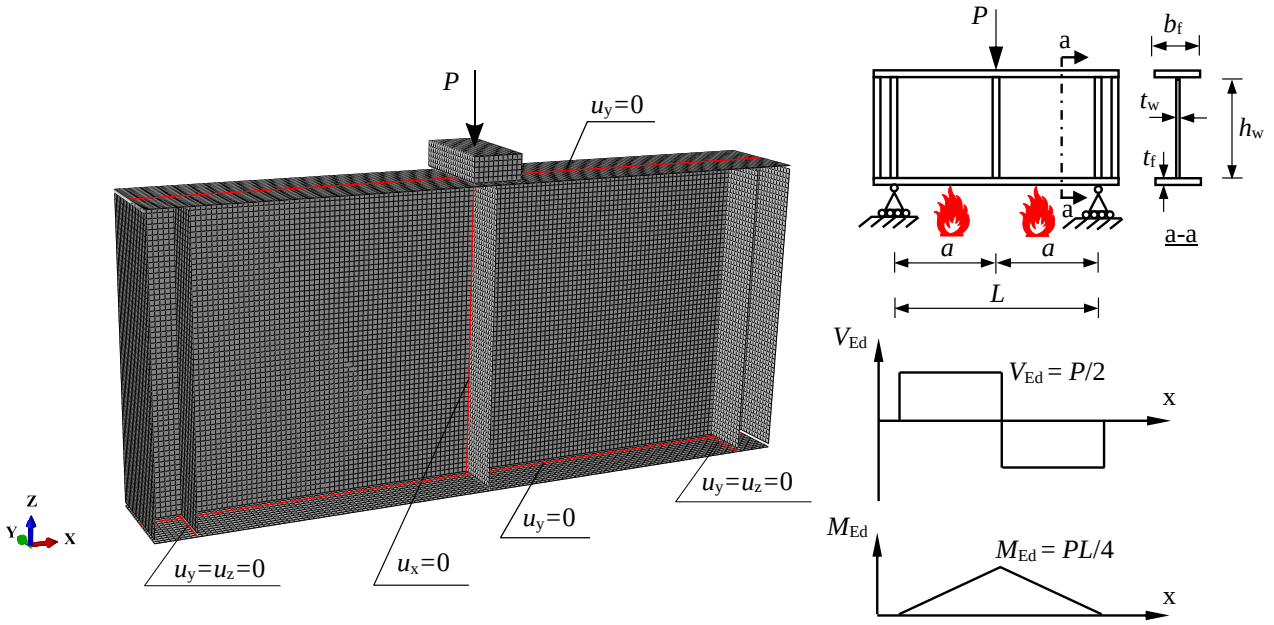

(a) Rigid end post

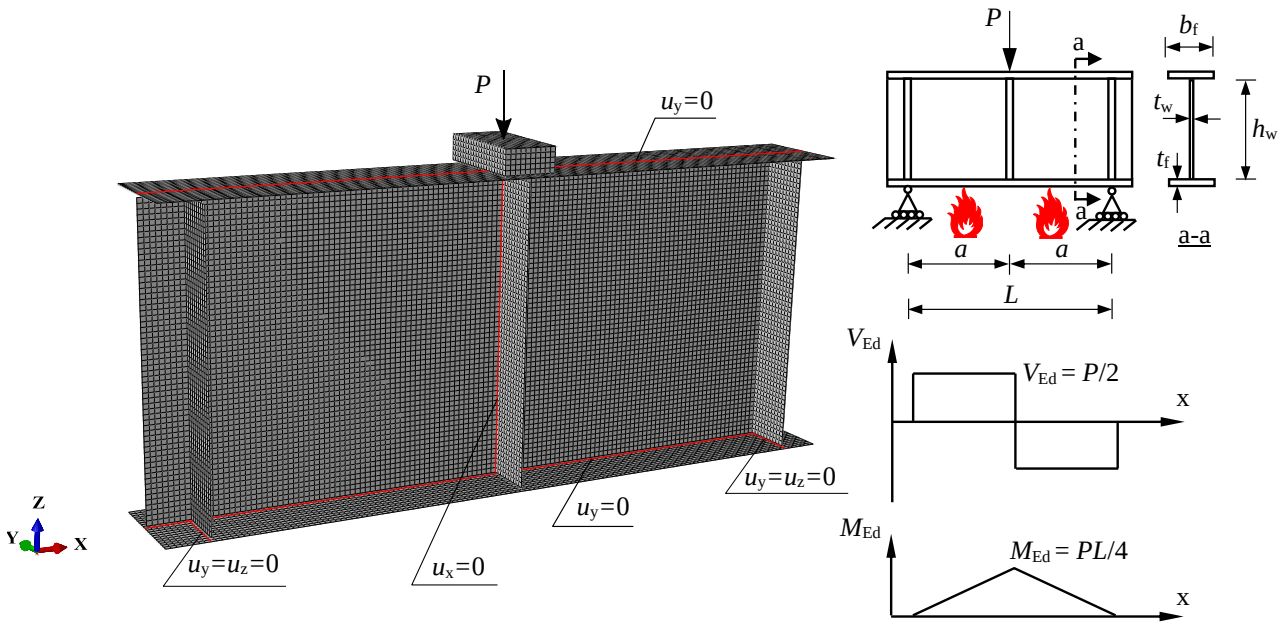

(b) Non-rigid end post

Figure 1: Boundary and loading conditions of the finite element model of stainless steel plate girders

figure, the translations u of the nodes within the bottom flange are restrained in the y and z directions (i.e. $u_y = u_z = 0$) at the supports, while the translations of the nodes within the web at the midspan are restrained in the x direction (i.e. $u_x = 0$). The overlapping of the web and flange plates was prevented by offsetting the web plates half the flange thicknesses and connecting the web and flange plates by means of rigid coupling beams as shown in Fig. 2. As can be seen from the figure, the web and flange plates were connected by means

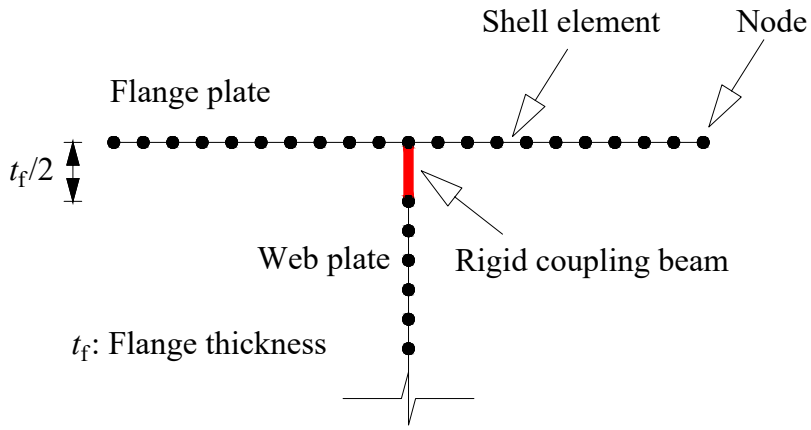

Figure 2: Use of rigid coupling beams for the connection of the web and flange plates of the modelled cross-sections of stainless steel plate girders

of rigid beam coupling, thereby accurately representing the cross-section properties without any artificial overpredictions of the cross-section strengths and stiffnesses which can result from the overlapping of the web and flange plates at the web-to-flange junctions. The same approach adopted in the modelling of the cross-sections of the stainless steel plate girders in this paper was also used in Boissonnade and Somja [37], Taras and Greiner [38] and Kucukler et al. [39], where its accuracy in the representation of the cross-section response of steel I-sections was verified. To avoid the lateral-torsional buckling of the analysed stainless steel plate girders, the translations of the nodes at the centroids of the top and bottom flanges are also restrained in the y direction along the lengths (i.e. $u_y = 0$). The loading P is applied to the finite element models by means of a rigid block at the mid-span as illustrated in Fig. 1, which generated uniform shear force $V_{Ed} = P/2$ along the span. The models were, of course, also under major axis bending moments whose maximum values were equal to $M_{Ed} = PL/4$ where L is the span length. The point force P is applied to the rigid block which transferred the applied loading to the analysed stainless steel girder; note that this procedure was utilised on the basis of the loading procedure adopted in physical experiments performed on stainless steel plate girders in the literature [4]. Shell-to-solid coupling was defined between the rigid block and the top surface of the top flange of the plate girder in accordance with Saliba and Gardner [40], thereby enabling the transfer of the applied load from the rigid block to the plate girder at the midspan. With the aim of avoiding web crushing, web crippling and web buckling effects, stiffener plates were utilised (i) at the midspan where the loading is applied and (ii) at the supports. Stiffener plates were also used at the ends of the plate girders with rigid end posts. More information

regarding the geometric properties of the stiffeners as well as the geometric properties of the analysed stainless steel plate girders such as the distances between stiffener plates a and the cross-section properties (i.e. the web height h_w, flange width b_f, web thickness t_w and flange thickness t_f) can be found in Section 2.3.

With the aim of mimicking the structural response of stainless steel girders in fire, the room temperature material response was modified by means of the elevated temperature strength and stiffness reduction factors set out in the Steel Construction Institute (SCI) Design Manual for Stainless Steel [41]. Grade 1.4301 austenitic and grade 1.4462 duplex stainless steel grades were taken into account to represent the common austenitic and duplex stainless steel grades. The elevated temperature stress-strain response was defined through a two-stage Ramberg-Osgood material model [42, 43] as provided by eqs. (1) and (2):

$$\epsilon = \frac{\sigma}{E_\theta} + 0.002\left(\frac{\sigma}{f_{p0.2,\theta}}\right)^{n_\theta} \quad \text{for} \quad \sigma \leq f_{p0.2,\theta}, \tag{1}$$

$$\epsilon = \frac{\sigma - f_{p0.2,\theta}}{E_{p0.2,\theta}} + \left(\epsilon_{u,\theta} - \epsilon_{p0.2,\theta} - \frac{f_{u,\theta} - f_{p0.2,\theta}}{E_{p0.2,\theta}}\right)\left(\frac{\sigma - f_{p0.2,\theta}}{f_{u,\theta} - f_{p0.2,\theta}}\right)^{m_\theta} + \epsilon_{p0.2,\theta} \quad \text{for} \quad f_{p0.2,\theta} < \sigma \leq f_{u,\theta}, \tag{2}$$

in which σ and ϵ are the stress and strain, $f_{p0.2,\theta}$ is the 0.2% proof strength at temperature θ, E_θ is the Young's modulus at temperature θ, $E_{p0.2,\theta}$ is the tangent modulus at $f_{p0.2,\theta}$, $\epsilon_{0.2,\theta}$ is the total strain corresponding to $f_{p0.2,\theta}$ and $f_{u,\theta}$ is the ultimate strength at temperature θ. In eqs. (1) and (2), n_θ and m_θ are the Ramberg-Osgood exponents that defines the nonlinearity of the material response. The 0.2% proof strength $f_{p0.2,\theta}$ at temperature θ and the ultimate strength $f_{u,\theta}$ at temperature θ were determined through multiplying their ambient temperature values f_y and f_u by the corresponding material reduction factors $k_{p0.2,\theta}$ and $k_{u,\theta}$ provided in [41] respectively, i.e. $f_{p0.2,\theta} = k_{p0.2,\theta} f_y$ and $f_{u,\theta} = k_{u,\theta} f_u$. The ambient temperature values of the 0.2% proof strength f_y and the ultimate tensile strength f_u were assumed as those put forward in [44] for hot-finished austenitic and duplex stainless steel plates. In line with [41], the elevated temperature ultimate strains $\epsilon_{u,\theta}$ were determined as

$$\epsilon_{u,\theta} = k_{\epsilon_{u,\theta}}\left(1 - \frac{f_y}{f_u}\right), \tag{3}$$

where $k_{\epsilon_{u,\theta}}$ is the elevated temperature ultimate strain reduction factor obtained from [41]. The elasticity modulus E_θ at temperature θ were determined by multiplying the elasticity modulus reduction factor $k_{E,\theta}$ given in [41] by the room temperature elasticity modulus E which was assumed as equal to 200 GPa (i.e. $E_\theta = k_{E,\theta} E$). In accordance with [41], the Ramberg-Osgood exponents n_θ utilised in eq. (1) were assumed to be equal to their room temperature values put forward in [44], whereas the values of the Ramberg-Osgood exponents m_θ employed in eq. (2) were calculated through the following equation [45]:

$$m_\theta = \frac{ln\left[\frac{\epsilon_{u,\theta} - \epsilon_{p0.2,\theta}(f_{u,\theta} - f_{p0.2,\theta})/E_{p0.2,\theta}}{0.02 - \epsilon_{p0.2,\theta}(f_{2,\theta} - f_{p0.2,\theta})/E_{p0.2,\theta}}\right]}{ln\left(\frac{f_{u,\theta} - f_{p0.2,\theta}}{f_{2,\theta} - f_{p0.2,\theta}}\right)} \quad \text{but} \quad 1.50 \leq m_\theta \leq 5.00, \tag{4}$$

in which $f_{2,\theta}$ is the elevated temperature material strength at 2% total strain at temperature θ which is calculated by multiplying the 2% elevated temperature strength reduction factor $k_{2,\theta}$ provided in [41] by the 0.2% proof strength at room temperature for hot-rolled stainless steel plates recommended in [44], i.e. $f_{2,\theta} = k_{2,\theta} f_y$. The utilisation of m_θ determined as given by eq. (4) enables the elevated temperature stress-strain curves pass through the elevated temperature 0.2% proof strength $f_{p0.2,\theta}$, elevated temperature strength at 2% total strain $f_{2,\theta}$ and the elevated temperature ultimate strength $f_{u,\theta}$ at the corresponding 0.2% proof strain, 2% total strain and ultimate strain values. The elevated temperature stress-strain curves and the elevated temperature material reduction factors used for the austenitic and duplex stainless steel plate girders in this study are shown in Fig. 3.

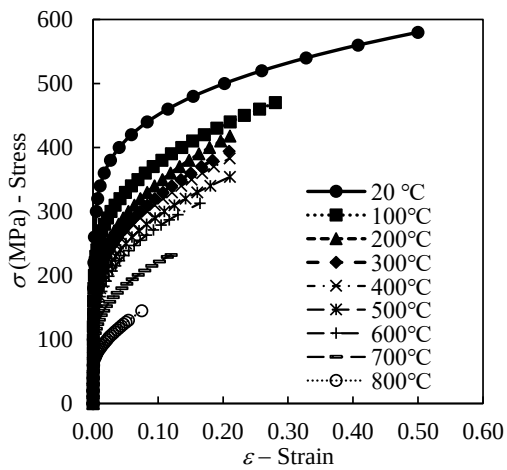

(a) Austenitic stainless steel elevated temperature stress-strain curves

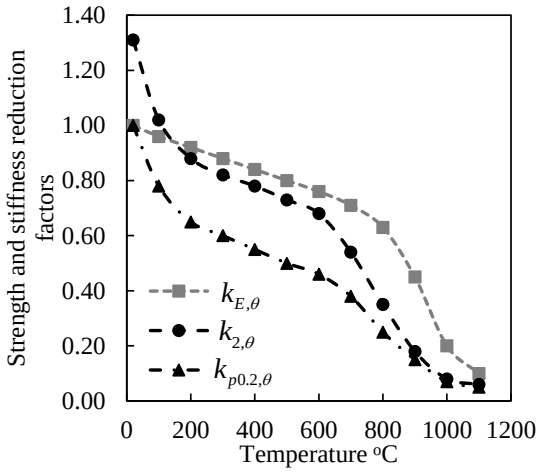

(b) Austenitic stainless steel elevated temperature material reduction factors

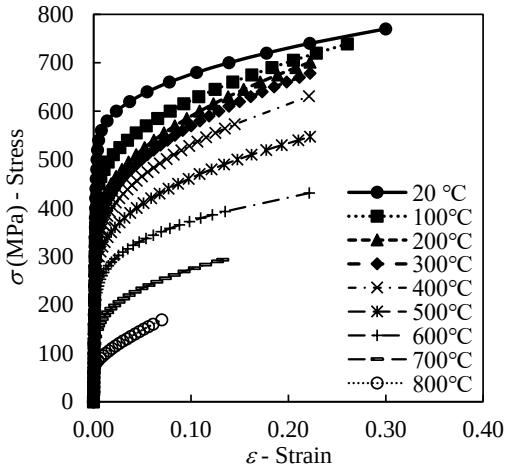

(c) Duplex stainless steel elevated temperature stress-strain curves

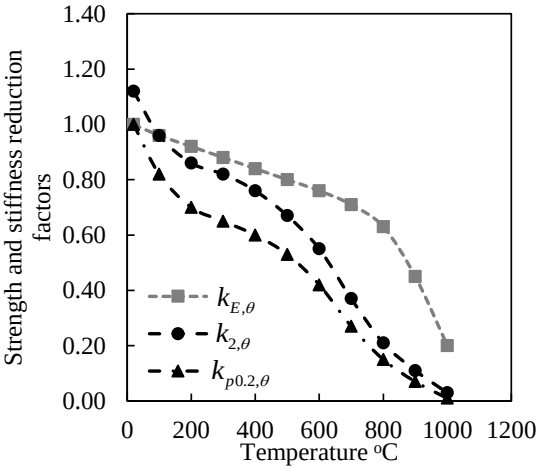

(d) Duplex stainless steel elevated temperature material reduction factors

Figure 3: Elevated temperature stress-strain curves and material reduction factors used in the finite element models of austenitic and duplex stainless steel girders in this study

It should be noted that the described elevated material modelling approach adopted in this paper for stainless steel has been incorporated into the upcoming version of the European structural steel fire design standard prEN 1993-1-2 [46] for the material modelling of stainless steel in fire, including (i) the two-stage Ramberg-Osgood material model given by eqs. (1) and (2) with the adopted n_θ and m_θ provided by eq. (4) as well as (ii) the material reduction factors $k_{2,\theta}$, $k_{p0.2,\theta}$, $k_{u,\theta}$ and $k_{E,\theta}$ recommended by [41] and used in this study. Thus, the elevated temperature material modelling technique adopted in this paper is in accordance with the elevated temperature material modelling approach recommended by the upcoming version of the European structural steel fire design standard prEN 1993-1-2 [46] for stainless steel.

Assuming that the considered stainless steel plate girders were fabricated through the welding of individual hot-finished austenitic and duplex stainless steel plates, the residual stress pattern proposed in [47] and shown in Fig. 4 was utilised in the application of the residual stresses to the finite element models. As can be seen from Fig. 4, the maximum

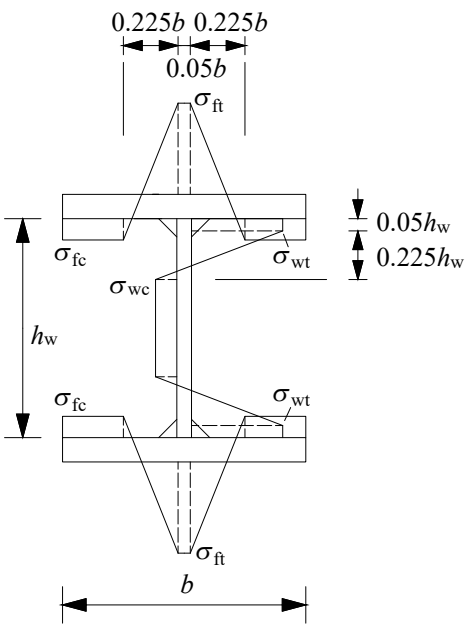

Figure 4: Residual stress pattern applied to the finite element models

values of the tensile residual stresses within the web σ_{wt} and flanges σ_{ft} are equal to 80% of the 0.2% proof stress f_y for austenitic stainless steel plate girders and 60% of the 0.2% proof stress f_y for duplex stainless steel plate girders, i.e. $\sigma_{wt} = \sigma_{ft} = 0.8f_y$ for austenitic stainless steel plate girders and $\sigma_{wt} = \sigma_{ft} = 0.6f_y$ for duplex stainless stainless steel plate girders. The axial force equilibrium is utilised in the calculation of the maximum compressive residual stresses within the web and flanges as recommended in [47]. It should be noted that as indicated in Saliba and Gardner [4], residual stresses do not have a significant influence on the shear resistances of stainless steel plate girders. Moreover, residual stresses within steel sections dissipate at elevated temperatures owing to the development of thermal strains

[34, 48]. However, even though their influence is expected to be largely immaterial, residual stresses were still included in the finite element models (i) for a realistic representation of the actual properties of stainless steel plate girders and (ii) considering the fact that they might have some small influence on the resistances of stainless steel plate girders undergoing bending dominant failure modes at relatively low elevated temperature levels (e.g. 300°C).

In the application of the geometric imperfections, the lowest local buckling modes obtained from the Linear Buckling Analyses of the finite element models were utilised, which were scaled to 80% of the fabrication tolerances provided in EN 1090-2 [49] for welded steel I-sections in line with the recommendations of EN 1993-1-5 [50]. Examples of local buckling modes for stainless steel plate girders with highly slender webs and the adopted local imperfection magnitudes $e_{o,w}$ and $e_{o,f}$ are shown in Fig. 5. Note that based upon the location

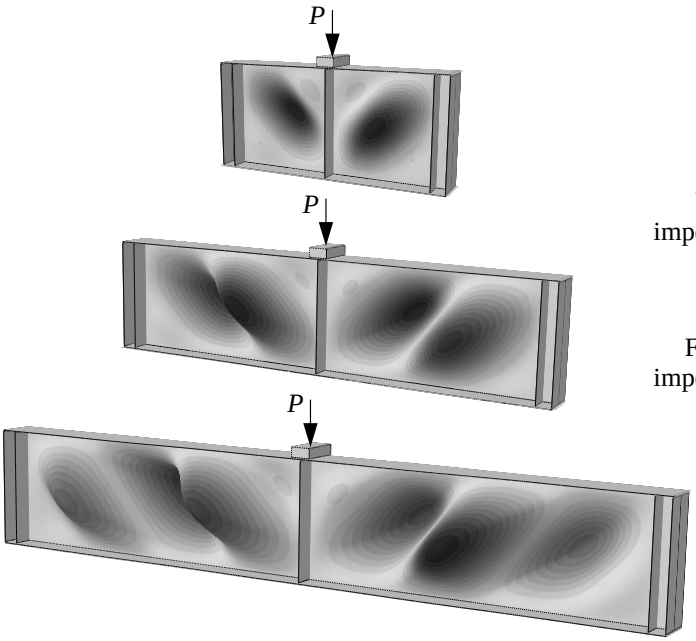

Web imperfection

$$e_{0,\mathrm{w}} = \begin{cases} 0.8h_w / 200 & \text{if} \quad h_w / t_w \le 80 \\ \dfrac{0.8h_w^2}{16000t_w} & \text{if} \quad 80 < h_w / t_w \le 200 \\ 0.8h_w / 80 & \text{if} \quad h_w / t_w > 200 \end{cases}$$

$$e_{0,\mathrm{w}} \ge 0.8t_{\mathrm{w}}$$

Flange imperfection

$$e_{0,\mathrm{f}} = \begin{cases} 0.8b_f / 150 & \text{if} \quad b_f / t_f \le 20 \\ 0.8b_f^2 / (3000t_f) & \text{if} \quad b_f / t_f > 20 \end{cases}$$

Figure 5: Geometric imperfection magnitudes e_0 and examples of local buckling modes for stainless steel plate girders with slender webs

(i.e. web or flange) of the largest normalised displacement observed in a Linear Buckling Analysis (LBA), the local buckling mode from the LBA was scaled using either the web imperfection magnitude $e_{o,w}$ (if the largest normalised displacement is observed in the web) or the flange imperfection magnitude $e_{o,f}$ (if the largest normalised displacement is observed in the flange). In the majority of the cases, the former was observed. As previously indicated, EN 1993-1-5 [50] recommends the use of 80% of the fabrication tolerances provided in EN 1090-2 [49] in the definition of local geometric imperfections in the finite element modelling of structural steel elements, which was adopted in this study. Note that the same approach used in this paper in the definition of the magnitudes of local geometric imperfections was also adopted in Chacon et al. [51, 52] and Fortan et al. [8] in their finite element modelling of the structural response of steel plate girders.

In the analysis of the finite element models, an isothermal analysis technique was adopted, where (i) the residual stresses were applied to the finite element models at room temperature, (ii) then, the temperatures of the finite element models were uniformly increased to predefined elevated temperature magnitudes θ resulting in the modification of the material stress-strain response as illustrated in Fig. 3 as well as the development of thermal strains and (iii) finally, the loading was applied to the finite element models at the designated elevated temperature levels θ. The modified Riks method was adopted in the final step so that the full load-deformation response of the finite element models could be determined including the post-ultimate response. Owing to the adoption of the isothermal analysis technique, the peak loads obtained from the finite element analyses were directly utilised as the ultimate load carrying capacities of the plate girders in line with the similar studies from the literature [53–55].

2.2. Validation of finite element models

In this subsection, the shell finite element of stainless steel plate girders are validated against experimental results from the literature. Since there is currently no experimental study performed on stainless steel plate girders at elevated temperatures in the literature, (i) the results from the experiments performed on carbon steel plate girders in fire by Vimonsatit et al. [56] and (ii) the results from the physical tests carried out on stainless steel plate girders at room temperature by Saliba and Gardner [4] and Chen et al. [6] are utilised for the validation of the finite element modelling approach adopted in this paper.

2.2.1. Vimonsatit et al. [56] experiments on carbon steel plate girders in fire

In Vimonsatit et al. [56], a series of fire experiments on carbon steel plate girders were performed, which are utilised for the validation of the finite element modelling approach adopted in this paper. The specimens were tested at room temperature and at 400 °C, 550 °C and 700 °C. An isothermal testing method was adopted in the experiments where the specimens were first heated up to a designated temperature and then loaded up to failure. The room temperature material properties of the specimens were obtained through a series of material tests in [56]. Using the room temperature material models measured in [56], (i) the elevated temperature material models of the specimens were created through the EN 1993-1-2 [9] elevated temperature material model and material reduction factors for carbon steel as recommended in [56] and (ii) adopted in the finite element models of the specimens created in this study. Some specimens of [56] represented typical column web panels under shear loading while the others represented the shear behaviour of plate girders; the specimens represented the shear behaviour of plate girders are utilised herein. The tested specimens had rigid end posts. The ultimate resistances of the plate girders obtained from the experiments of [56] $V_{u,test}$ and those determined through the finite element models $V_{u,FE}$ are compared in Table 1 for different elevated temperature levels. The web height h_w and thickness t_w as well as the unstiffened length a to web height h_w (a/h_w) ratios of the specimens are also illustrated in Table 1. As can be seen from the table, the ultimate resistances of the plate girders determined through the finite element models $V_{u,FE}$ correlate well with those observed in the experiments of [56] $V_{u,test}$ at different elevated temperature

Table 1: Comparison of the ultimate shear loads of the carbon steel plate girders observed in the fire experiments of Vimonsatit et al. [56] $V_{u,test}$ and those obtained from the finite element models created in this study $V_{u,FE}$

Specimen	Temperature (°C)	h_w (mm)	t_w (mm)	a/h_w	$V_{u,test}$ (kN)	$V_{u,FE}$ (kN)	$V_{u,FE}/V_{u,test}$
TG3-1	20	305	2	1	79.95	76.28	0.96
TG3-2	400	305	2	1	67.63	64.72	0.96
TG3-3	565	305	2	1	34.34	37.87	1.10
TG3-4	700	305	2	1	17.15	16.48	0.96
TG5-1	20	305	1.5	1	59.6	57.85	0.97
TG5-2	400	305	1.5	1	46.4	46.18	1.00
TG5-3	550	305	1.5	1	28.6	29.31	1.02
TG5-4	700	305	1.5	1	10.16	10.64	1.05
						Average	1.00
						COV	0.053

levels, highlighting that the finite element models created in this paper are able to replicate the structural response of steel plate girders influenced by shear buckling and local buckling effects in fire.

2.2.2. Saliba and Gardner [4] and Chen et al. [6] experiments on stainless steel plate girders at room temperature

Saliba and Gardner [4] and Chen et al. [6] performed a series of experiments on austenitic and duplex stainless steel plate girders at room temperature with rigid and non-rigid end posts as well as different unstiffened length a to web height h_w (i.e. a/h_w) ratios. The tested stainless steel plate girders were subjected to point loads at their mid-spans and had roller supports. The material properties of the tested specimens were obtained by means of a series of coupon tests in [2, 4], which were utilised in the finite element models created herein. In Table 2, the ultimate shear loads $V_{u,test}$ of the specimens observed in the physical tests of [4, 6] and the ultimate shear loads $V_{u,FE}$ obtained by means of the finite element models of the specimens created herein are compared. As can be seen from the table, there is a good agreement between the ultimate shear loads of the austenitic and duplex stainless steel plate girders obtained from the finite element models $V_{u,FE}$ and those observed in the experiments $V_{u,test}$ for different web height h_w to web thickness t_w ratios (i.e. h_w/t_w) as well as different unstiffened length a to web height h_w ratios (i.e. a/h_w), which indicates that the finite element models are able to accurately estimate the behaviour of stainless steel plate girders susceptible to shear and local buckling effects. In Fig. 6, the applied load P versus mid-span displacement paths δ of the specimens observed in the experiments of Saliba and Gardner [4] and those obtained from the finite element models created in this study are compared. As can be seen from the figure, the experimental and numerical applied load versus mid-span displacement paths are in close agreement, highlighting that the finite element models are capable of mimicking the structural response of stainless steel plate girders. It should be

Table 2: Comparison of the ultimate shear loads of the stainless steel plate girders observed in the experiments of Saliba and Gardner [4] and Chen et al. [6] $V_{u,test}$ and those obtained from the finite element models created in this study $V_{u,FE}$

Study	Specimen	End post	h_w (mm)	t_w (mm)	a/h_w	$V_{u,test}$ (kN)	$V_{u,FE}$ (kN)	$V_{u,FE}/V_{u,test}$
Saliba and Gardner [4]	I-600×200×12×10-1	Rigid	600	10	1.0	1838	1824	0.99
	I-600×200×12×8-1	Rigid	600	8	1.0	1326	1292	0.97
	I-600×200×12×6-1	Rigid	600	6	1.0	888	894	1.01
	I-600×200×12×4-1	Rigid	600	4	1.0	562	579	1.03
	I-600×200×15×15-2	Rigid	600	15	2.0	1801	1773	0.98
	I-600×200×12×10-2	Rigid	600	10	2.0	1162	1195	1.03
	I-600×200×12×8-2	Rigid	600	8	2.0	976	951	0.97
	I-600×200×12×6-2	Rigid	600	6	2.0	682	689	1.01
	I-600×200×12×4-2	Rigid	600	4	2.0	396	409	1.03
Chen et al. [6]	V-304-300ad1	Non-rigid	300	4	1.0	253.2	244.1	0.96
	V-304-500ad1.5	Non-rigid	500	4	1.5	243.2	238.3	0.98
	V-304R500ad1	Rigid	500	4	1.0	322.2	311.6	0.97
	V-2205-500ad1	Non-rigid	500	4	1.0	453.9	457.5	1.01
	V-2205-500ad1.5	Non-rigid	500	4	1.5	385.9	395.1	1.02
	V-2205-R500ad1	Rigid	500	4	1.0	512.7	533.2	1.04
							Average	1.00
							COV	0.026

noted that in addition to the validation studies presented in this subsection, the adopted finite element modelling approach has also been validated for carbon steel and stainless steel columns, beams and cross-sections at elevated temperatures in Kucukler [34, 35], Kucukler et al. [57] and Xing et al. [58].

2.3. Parametric studies

Table 3 shows a summary of the numerical parametric studies carried out in this paper. As can be seen from the table, stainless steel plate girders with both rigid and non-rigid end posts were taken into consideration. The web height h_w and flange width b were taken as equal to 600 mm and 200 mm for all the stainless steel grades respectively (i.e. $h_w = 600$ mm and $b = 200$ mm), which was in line with the values adopted in the experiments of Saliba and Gardner [4]. For the case of the flange thicknesses t_f, three values of 15 mm, 12 mm and 10 mm were considered (i.e. $t_f = 15, 12$ and 10 mm). With the aim of obtaining a broad range of web slendernesses for the investigated stainless steel plate girders, 7 different web thickness t_w values equal to 10 mm, 8 mm, 6 mm, 4 mm, 3 mm, 2.5 mm and 2 mm were taken into account (i.e. $t_w = 10, 8, 6, 4, 3, 2.5$ and 2 mm). Four different unstiffened length a to web height h_w ratios equal to 0.5, 1.0, 2.0 and 3.0 were considered (i.e. a/h_w=0.5, 1.0, 2.0, 3.0). It should be noted that as can be seen from Table 3, for the case of the plate girders with a/h_w ratios equal to 0.5, additional stiffener plates between those at the supports and mid-span were utilised; also, the flange thickness t_f equal to 15 mm (i.e. $t_f = 15$ mm) was

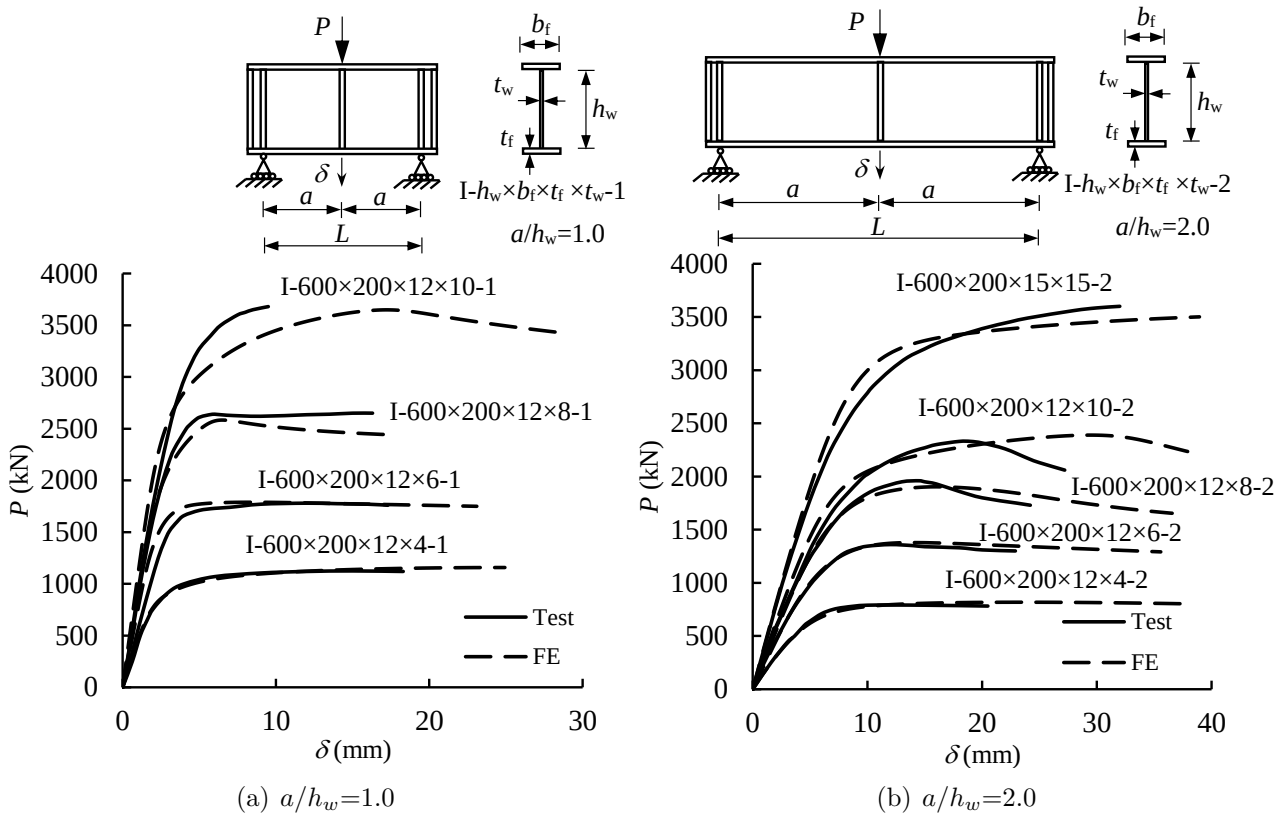

(a) a/h_w=1.0 (b) a/h_w=2.0

Figure 6: Comparison of the load versus mid-span displacement paths observed in the experiments of Saliba and Gardner [4] and those obtained from the shell finite element models created in this study

used for these plate girders. Both austenitic and duplex stainless steel girders were taken into consideration. For the purpose of exploring the structural response of stainless steel plate girders subjected to a broad spectrum of elevated temperature levels, five different elevated temperature values θ equal to 300° C, 400° C, 500° C, 600° C and 700° C were considered (i.e. θ=300° C, 400° C, 500° C, 600° C and 700° C). Taking into account the wide range of parameters shown in Table 3, nonlinear finite element analyses of 700 stainless steel plate girders in fire were carried out in this study, which furnished comprehensive structural performance data on the structural performance of stainless steel plate girders at elevated temperatures. This comprehensive structural performance data is utilised in the following sections of this paper for (i) the assessment of the accuracy of EN 1993-1-4 [9] applied with the elevated temperature material properties of stainless steel and (ii) the establishment of new design rules providing accurate and safe estimations of the behaviour of stainless steel plates in fire.

It is worthwhile indicating that the additional intermediate stiffeners were employed in the stainless steel plate girders with the a/h_w ratio of 0.5 as shown in Table 3 to assess the contribution of using intermediate stiffeners between the supports and the load application points at the midspan. Since EN 1993-1-4 [10] does not include any clause preventing the use of intermediate stiffeners between the load application points and supports within

Table 3: Summary of numerical parametric studies performed on stainless steel plate girders in fire

Geometry & loading	h_w (mm)	b_f (mm)	t_f (mm)	t_w (mm)	a/h_w	Stainless steel grades	Temperature θ
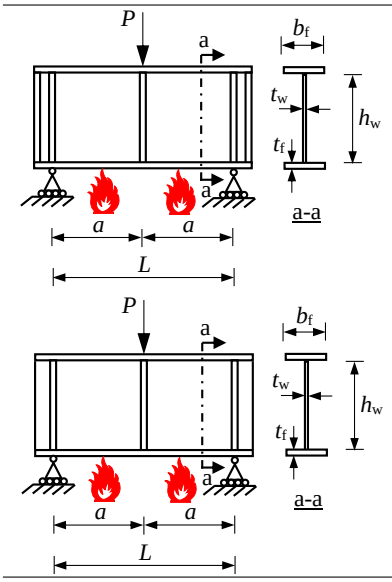	600	200	15 12 10	10 8 6 4 3 2.5 2	1.0 2.0 3.0	Austenitic Duplex	300° C 400° C 500° C 600° C 700° C
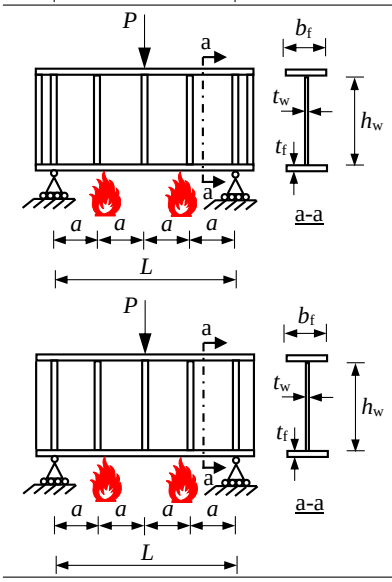	600	200	15	10 8 6 4 3 2.5 2	0.5	Austenitic Duplex	300° C 400° C 500° C 600° C 700° C

stainless steel plate girders, it was assumed that the design resistance predictions obtained through EN 1993-1-4 [10] can be utilised to predict the ultimate resistances of stainless steel plate girders with intermediate stiffeners. It should be noted that Reis et al. [53] also used intermediate stiffeners between the load application points and supports in their numerical models whose results were used in the assessment of EN 1993-1-5 [50] for the predictions of the ultimate resistances of carbon steel plate girders at elevated temperatures.

3. Assessment of EN 1993-1-4 design rules applied with elevated temperature material properties of stainless steel

Since the European structural steel fire design standard EN 1993-1-2 [9] does not involve specific fire design methods for stainless steel plate girders, the accuracy of the European structural stainless steel design standard EN 1993-1-4 [10] applied with the elevated temperature material properties of stainless steel is assessed for the fire design of stainless steel plate girders in this section. Initially, the EN 1993-1-4 [10] room temperature design rules for stainless steel plate girders are briefly set out. Then, their accuracy when applied with the elevated material properties of stainless steel is assessed against comprehensive numerical structural performance data obtained through the validated finite element models in the previous section.

3.1. EN 1993-1-4 design rules for stainless steel plate girders

EN 1993-1-4 [10] provides the following expression for the determination of the shear resistances $V_{b,Rd}$ of stainless steel plate girders which is the sum of the web shear buckling resistance $V_{bw,Rd}$ and the flange contribution $V_{bf,Rd}$:

$$V_{b,Rd} = V_{bw,Rd} + V_{bf,Rd} \leq \frac{\eta f_{yw} h_w t_w}{\sqrt{3}\gamma_{M1}}, \tag{5}$$

in which η is a parameter approximating the influence of the strain hardening equal to 1.2 (i.e. $\eta = 1.2$), f_{yw} is the 0.2% proof strength of the web, γ_{M1} is the partial safety factor, h_w is the web height and t_w is the web thickness. The web shear buckling resistance $V_{bw,Rd}$ can be determined using the following expression:

$$V_{bw,Rd} = \frac{\chi_w f_{yw} h_w t_w}{\sqrt{3}\gamma_{M1}}, \tag{6}$$

where χ_w is the web shear buckling reduction factor. The flange contribution $V_{bf,Rd}$ is calculated as:

$$V_{bf,Rd} = \left(\frac{b_f t_f^2 f_{yf}}{c\gamma_{M1}}\right)\left[1 - \left(\frac{M_{Ed}}{M_{f,Rd}}\right)^2\right], \tag{7}$$

where M_{Ed} is the bending moment affecting the shear girder, $M_{f,Rd}$ is the bending moment resistance of the cross-section determined considering the flanges only, b_f is the flange width, t_f is the flange thickness, f_{yf} is the 0.2% proof strength of the flanges and the distance c which specifies the location of the plastic hinges developing within the flanges is determined through the following equation:

$$c = \left(0.17 + \frac{3.5 b_f t_f^2 f_{yf}}{t_w h_w^2 f_{yw}}\right) a \quad \text{with} \quad \frac{c}{a} \leq 0.65. \tag{8}$$

The shear buckling reduction factor χ_w is determined as shown in Table 4 where $\overline{\lambda}_w$ is the

Table 4: Shear buckling reduction factors χ_w provided in EN 1993-1-4 [10] for stainless steel plate girders with rigid and non-rigid end posts

	χ_w for rigid end post	χ_w for non-rigid end post
$\overline{\lambda}_w \leq 0.65/\eta$	η	η
$0.65/\eta < \overline{\lambda}_w < 0.65$	$0.65/\overline{\lambda}_w$	$0.65/\overline{\lambda}_w$
$\overline{\lambda}_w \geq 0.65$	$1.56/(0.91 + \overline{\lambda}_w)$	$1.19/(0.54 + \overline{\lambda}_w)$

non-dimensional web slenderness calculated through the following expression:

$$\overline{\lambda}_w = \sqrt{\frac{f_{yw}/\sqrt{3}}{\tau_{cr}}} = \frac{h_w}{37.4 t_w \epsilon \sqrt{k_\tau}}, \tag{9}$$

where τ_{cr} is the elastic critical shear buckling stress that can be determined by means of the formulae provided in Annex A.3 of EN 1993-1-5 [50], k_τ is the shear buckling coefficient and ϵ is the material factor equal to $\epsilon = \sqrt{(235/f_{yw})\,(E/210000)}$.

3.2. Adoption of EN 1993-1-4 for the fire design of stainless steel plate girders

As previously stated, EN 1993-1-2 [9] does not provide specific fire design rules for stainless steel plate girders, which is also the case for the fire design of conventional carbon steel plate girders. Thus, in this study, the room temperature design rules provided in EN 1993-1-4 [10] for stainless steel plate girders were used in conjunction with the reduced material strength and stiffness at elevated temperatures for the fire design of stainless steel plate girders. The design equations provided in eqs. (5)-(9) were used in conjunction with the reduced material strengths and stiffness determined as

$$f_{yw,\theta} = k_{2,\theta} f_{yw}, \tag{10}$$

$$f_{yf,\theta} = k_{2,\theta} f_{yf}, \tag{11}$$

$$E_\theta = k_{E,\theta} E, \tag{12}$$

where $k_{2,\theta}$ is the elevated temperature strength reduction factor at 2% total strain, $f_{yw,\theta}$ and $f_{yf,\theta}$ are the web and flange elevated temperature material strengths at 2% total strain at temperature θ, $k_{E,\theta}$ is the elevated temperature elasticity modulus reduction factor and E_θ is the elevated temperature Young's modulus at temperature θ; $k_{2,\theta}$ and $k_{E,\theta}$ values for stainless steel provided in prEN 1993-1-2 [46] which were also used in the finite element modelling as described in Section 2.1 were utilised. Determined using the elevated temperature material properties of stainless steel (i.e. $f_{yw,\theta} = k_{2,\theta} f_{yw}, f_{yf,\theta} = k_{2,\theta} f_{yf}, E_\theta = k_{E,\theta} E$), the shear resistance of a plate girder at temperature θ can be denoted by $V_{b,Rd,\theta}$, the web shear buckling resistance at temperature θ can be denoted by $V_{bw,Rd,\theta}$ and the flange contribution to the shear resistance at temperature θ can be denoted by $V_{bf,Rd,\theta}$, while the bending moment resistance determined considering the flanges only at temperature θ can be denoted by $M_{f,Rd,\theta}$ for a stainless steel plate girder in fire. For stocky stainless steel plate girders, the strain hardening coefficient η is taken as 1.2 as recommended for room temperature design

as stainless steel can exhibit strain hardening in fire, exceeding the elevated temperature strengths at 2% total strains $f_{2,\theta} = k_{2,\theta} f_y$ (see Fig. 3).

It should be noted that considering that EN 1993-1-2 [9] also does not provide fire design rules for carbon steel plate girders, Reis et al. [53] also adopted a similar procedure followed in this paper by (i) utilising the elevated temperature material reduction factors $k_{2,\theta}$ and $k_{E,\theta}$ for carbon steel to determine the elevated temperature material strengths and stiffnesses (i.e. $f_{yw,\theta} = k_{2,\theta} f_{yw}$, $f_{yf,\theta} = k_{2,\theta} f_{yf}$ $E_\theta = k_{E,\theta} E$) and (ii) using the room temperature carbon steel plate girder design rules provided in EN 1993-1-5 [50] for the fire design of carbon steel plate girders. In line with [53], the bending moment resistances of the cross-sections determined considering the flanges only $M_{f,Rd,\theta}$ at temperature θ (see eq. (7)) were calculated using (i) the elevated temperature strengths at 2% total strain $f_{2,\theta} = k_{2,\theta} f_y$ for Class 1, 2 and 3 sections and (ii) 0.2% proof strengths $f_{p0.2,\theta} = k_{p0.2,\theta} f_y$ for Class 4 sections in the adoption of the room temperature design rules of EN 1993-1-4 [10] with the elevated temperature material strengths and stiffnesses in this paper. In the following subsection, the accuracy of the adopted approach for the fire design of stainless steel plate girders is assessed.

3.3. Accuracy assessment

The accuracy of EN 1993-1-4 [10] applied with the elevated temperature material properties as described in the previous subsection is shown in Fig. 7 for the ultimate web shear strength predictions of austenitic and duplex stainless steel plate girders with rigid and non-rigid posts in fire. In Fig. 7, the shear buckling reduction factors obtained by means of the Geometrically and Materially Nonlinear Analyses with Imperfections (GMNIA) of the finite element models $\chi_{w,\theta,GMNIA}$ are calculated as follows

$$\chi_{w,\theta,GMNIA} = \frac{V_{Ed,GMNIA} - \frac{b_f t_f^2 (k_{2,\theta} f_{yf}/\sqrt{3})}{c} \left[1 - \left(\frac{M_{Ed,GMNIA}}{M_{f,Rd,\theta}}\right)^2\right]}{(k_{2,\theta} f_{yw}/\sqrt{3}) h_w t_w}, \tag{13}$$

where $V_{Ed,GMNIA}$ and $M_{Ed,GMNIA}$ are the ultimate shear force and bending moment values within the stainless steel plate girders obtained from the GMNIA, respectively. It should be noted that eq. (13) was simply obtained by expressing eq. (5) in terms of χ_w and utilising maximum shear $V_{Ed,GMNIA}$ and bending moment resistances $M_{Ed,GMNIA}$ obtained from the GMNIA. As can be seen from Fig. 7, the use of the EN 1993-1-4 [10] room temperature plate girder design rules with the elevated temperature stainless steel material properties leads to rather inaccurate web shear resistance predictions which can be on the unsafe side for stainless steel plate girders in fire. This observation is not surprising as the elevated temperature material response of stainless steel can be considerably different than its room temperature material response, thus leading to considerably different structural response of stainless steel plate girders in fire relative to their behaviour at ambient temperature.

As described in [4, 5], steel plate girders typically exhibit three primary failure modes which are (i) a shear dominant failure that involves the shear buckling of the web of the plate girder, (ii) a bending dominant failure mode that features the local buckling of the compression flange of the plate girder and (iii) a combined bending and shear failure mode

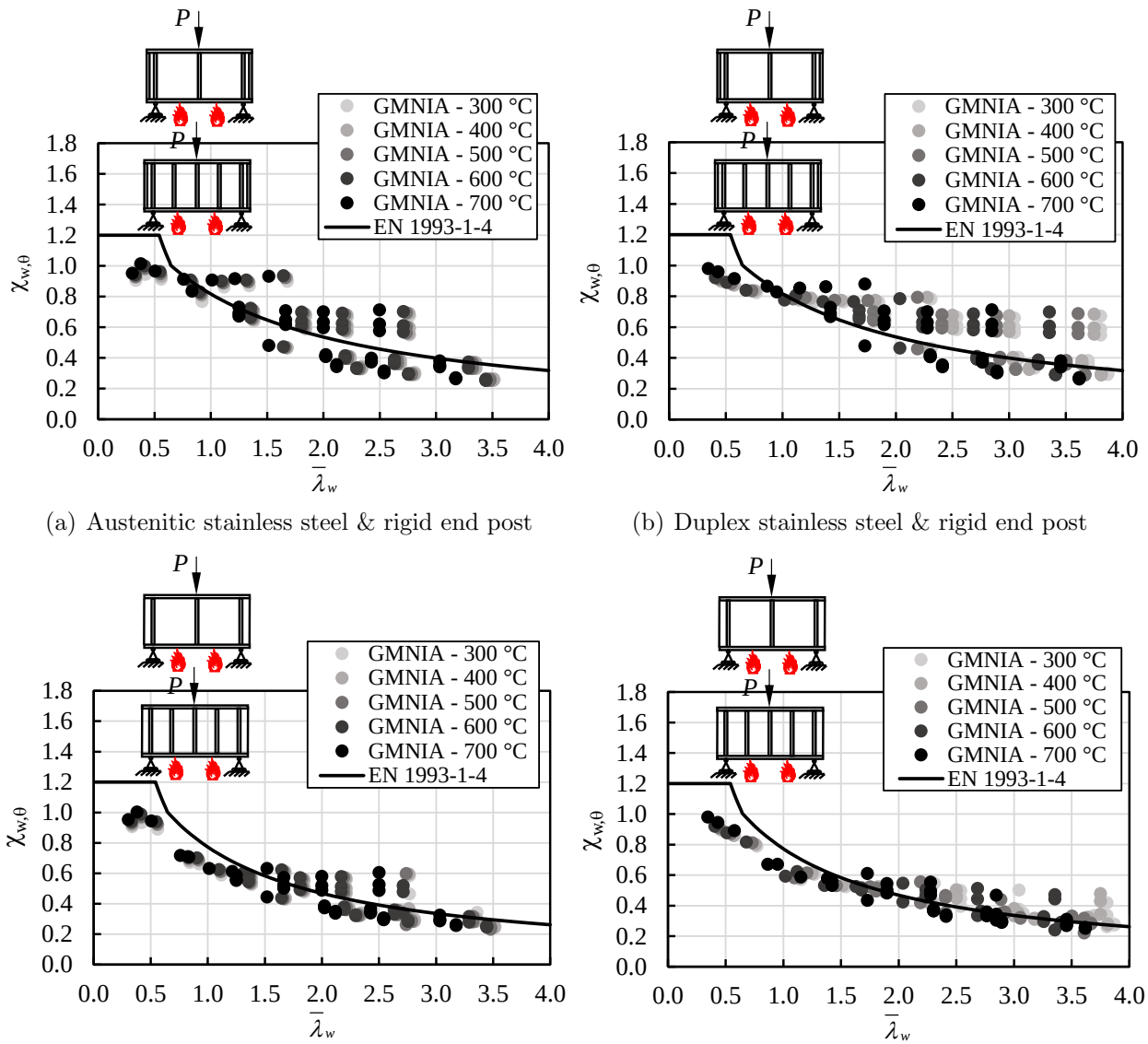

(a) Austenitic stainless steel & rigid end post

(b) Duplex stainless steel & rigid end post

(c) Austenitic stainless steel & non-rigid end post

(d) Duplex stainless steel & non-rigid end post

Figure 7: Accuracy of EN 1993-1-4 [10] applied with the elevated temperature material properties of stainless steel for the fire design of stainless steel plate girders undergoing a shear dominant failure mode

which features the interaction of the shear and bending failure modes. In the analysis of the data from the GMNIA in this study, two cases were taken into account: (i) Case 1 where the stainless steel plate girders feature a shear dominant failure mode with $V_{Ed,GMNIA}/M_{Ed,GMNIA} > V_{bw,Rd,\theta}/M_{f,Rd,\theta}$ and (i) Case 2 where the stainless steel plate girders exhibit a bending dominant failure mode and a combined bending and shear failure mode with $V_{Ed,GMNIA}/M_{Ed,GMNIA} \leq V_{bw,Rd,\theta}/M_{f,Rd,\theta}$. The described two cases taken into account in this study are shown in Fig. 8, where $M_{pl,Rd,\theta}$ is the design plastic resistance of the cross-section consisting of the effective area of the flanges and fully effective web irrespective of

its section class at temperature θ. The parameter ϕ in Fig. 8 is the radial angle describing

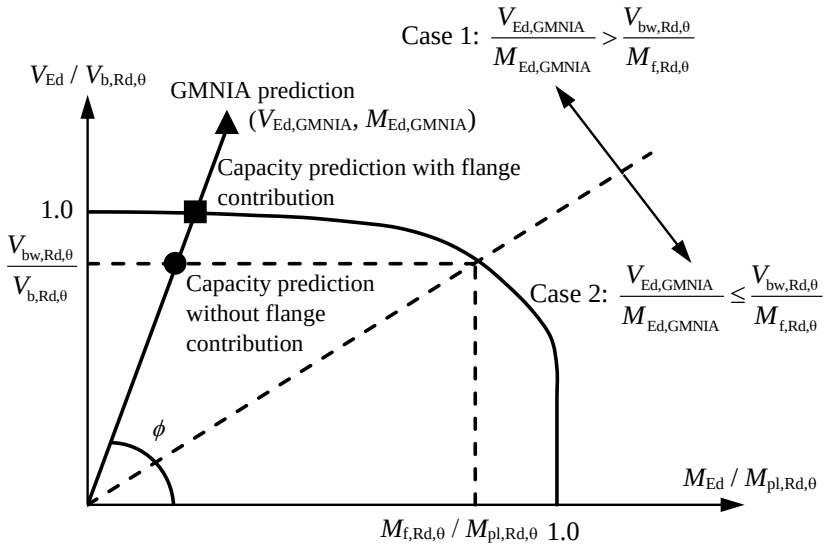

Figure 8: Normalised moment-shear interaction (M-V int.) diagram and description of Case 1 and Case 2

the relationship between the applied shear force and bending moment for a stainless steel plate girder and determined as

$$\phi = tan^{-1}\left[\frac{V_{Ed,GMNIA}/V_{b,Rd,\theta}}{M_{Ed,GMNIA}/M_{pl,Rd,\theta}}\right]. \tag{14}$$

For $\phi > tan^{-1}[(V_{bw,Rd,\theta}/V_{b,Rd,\theta})/(M_{f,Rd,\theta}/M_{pl,Rd,\theta})]$, the plate girder is subjected to a shear dominant failure mode which is classified as Case 1 in this study, while for $\phi \leq tan^{-1}[(V_{bw,Rd,\theta}/V_{b,Rd,\theta})/(M_{f,Rd,\theta}/M_{pl,Rd,\theta})]$, the plate girder is subjected to a bending dominant failure mode or a combined bending and shear failure mode which is classified as Case 2 in this study. Examples of a shear dominant failure mode (i.e. Case 1) as well as a bending dominant failure mode and a combined bending and shear failure mode (Case 2) are shown in Fig. 9. It should be emphasised that amongst all the stainless steel plate girders considered in the parametric studies described in Section 2.3, those subjected to a shear dominant failure mode (i.e. Case 1) are taken into account to assess the accuracy of the shear buckling rules of EN 1993-1-4 [10] applied with the elevated temperature material properties of stainless steel in Fig. 7. This is in line with the similar studies [5] on the behaviour and design of stainless steel plate girders.

The accuracy of EN 1993-1-4 [10] design rules for stainless steel plate girders applied with the elevated temperature material properties of stainless steel (i.e. $f_{yw,\theta} = k_{2,\theta} f_{yw}, f_{yf,\theta} = k_{2,\theta} f_{yf}, E_\theta = k_{E,\theta} E$) is also shown in Fig. 10 for both Case 1 (shear dominant) and Case 2 (bending dominant or combined bending and shear) failure modes, considering austenitic and duplex stainless steel plate girders with rigid and non-rigid end posts in fire. Note that the following equation was utilised in the consideration of shear and bending interaction for

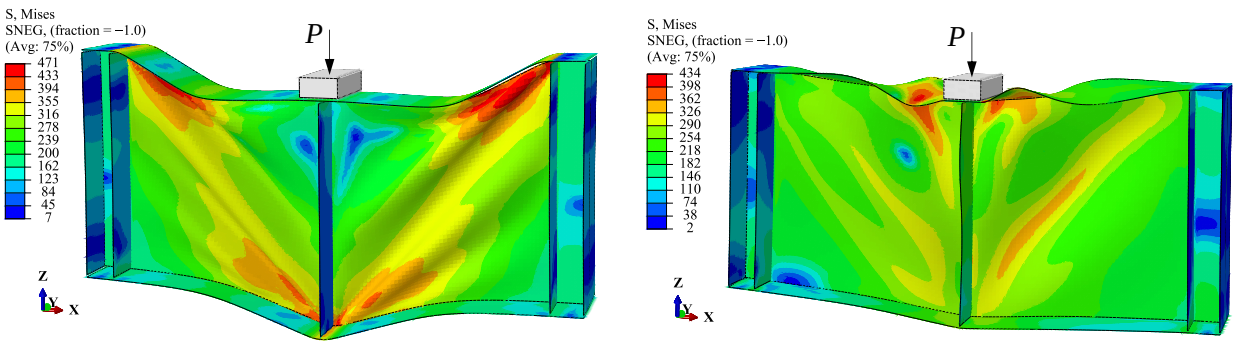

(a) Shear dominant failure mode

(b) Bending dominant failure mode

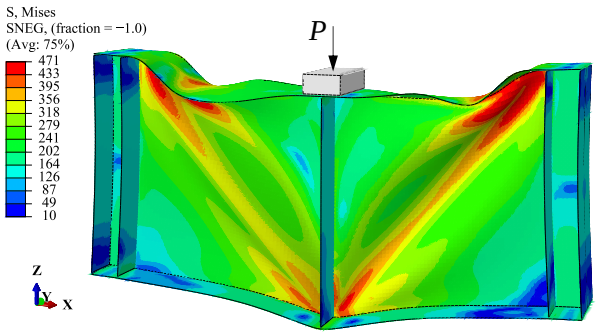

(c) Combined bending and shear failure mode

Figure 9: Examples of shear dominant, bending dominant and combined bending and shear failure modes (Stresses in MPa)

stainless steel plate girders as recommended in EN 1993-1-4 [10] and EN 1993-1-5 [50]:

$$\overline{\eta}_1 + \left(1 - \frac{M_{f,Rd,\theta}}{M_{pl,Rd,\theta}}\right)(2\overline{\eta}_3 - 1)^2 \leq 1.0 \quad \text{for} \quad \overline{\eta}_1 \geq \frac{M_{f,Rd,\theta}}{M_{pl,Rd,\theta}}, \tag{15}$$

in which $M_{pl,Rd,\theta}$ is the design plastic resistance of the cross-section consisting of the effective area of the flanges and fully effective web irrespective of its section class at temperature θ where the effective widths of the flanges were determined using the room temperature effective width design rules of EN 1993-1-4 [10]. In eq. (15), $\overline{\eta}_1$ is an auxiliary coefficient equal to

$$\overline{\eta}_1 = \frac{M_{Ed}}{M_{pl,Rd,\theta}}, \tag{16}$$

and $\overline{\eta}_3$ is another auxiliary coefficient determined as

$$\overline{\eta}_3 = \frac{V_{Ed}}{V_{bw,Rd,\theta}}. \tag{17}$$

Note that the normalised shear bending M-V interaction diagrams illustrated in Fig. 10 are created utilising eq. (15). In Fig. 10, M-V int. (av.), M-V int. (max.) and M-V int. (min.)

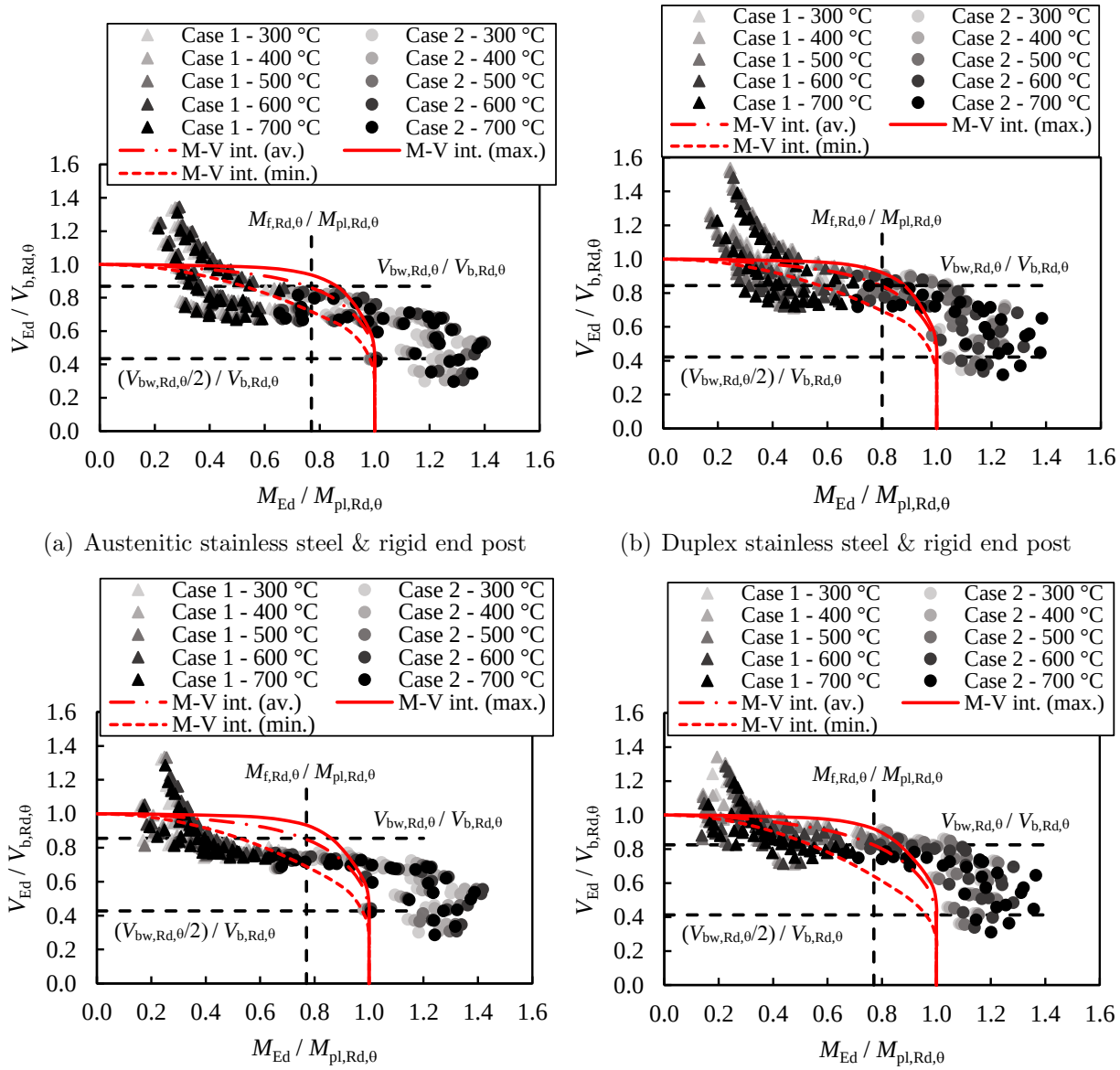

(a) Austenitic stainless steel & rigid end post

(b) Duplex stainless steel & rigid end post

(c) Austenitic stainless steel & non-rigid end post

(d) Duplex stainless steel & non-rigid end post

Figure 10: Normalised moment-shear interaction (M-V int.) diagrams obtained from EN 1993-1-4 [10] applied with the elevated temperature material properties and their accuracy against GMNIA for austenitic and duplex stainless steel plate girders with rigid and non-rigid end posts in fire

diagrams are obtained by taking the average, maximum and minimum of the data points of the normalised moment-shear M-V interaction diagrams created considering all the stainless steel plate girders taken into account in the numerical parametric studies shown in Table 3 for radial angle ϕ (see Fig. 8) values ranging between 0° and 90° with an increment size of 5°. Due to the dependency of the shapes of the normalised moment-shear M-V interaction diagrams on $V_{b,w,Rd,\theta}/V_{b,f,Rd,\theta}$ and $M_{f,Rd,\theta}/M_{pl,Rd,\theta}$ ratios, the normalised moment-shear M-V

interaction diagrams vary for each considered stainless steel plate girder in the parametric studies. Thus, there is not a single curve that can be used for accuracy assessment. The average M-V int. (av.), maximum M-V int. (max.) and minimum M-V int. (min.) normalised moment-shear M-V interaction diagrams provide a general assessment of the accuracy of the EN 1993-1-4 [10] stainless steel plate girder design rules applied with the elevated temperature material properties of stainless steel for stainless steel plate girders undergoing the (i) shear dominant failure modes (Case 1) and (ii) the bending dominant and combined bending and shear failure modes (Case 2) at elevated temperatures. As can be seen from Fig. 10, the use of the EN 1993-1-4 [10] design rules with the elevated temperature material properties of stainless steel generally leads to somewhat inaccurate ultimate strength predictions for stainless steel plate girders in fire, which can be quite unsafe in some cases.

The observations made in this section clearly indicate that the adoption of the room temperature EN 1993-1-4 [10] stainless steel plate girder design rules with the elevated temperature material properties of stainless steel is not appropriate for the design of stainless steel plate girders in fire, thus highlighting that new fire design rules for stainless steel plate girders is necessary. To address this necessity, new design rules for stainless steel plate girders in fire that are compatible with the design philosophies of EN 1993-1-2 [9], EN 1993-1-4 [10] and EN 1993-1-5 [50] are put forward in the next section.

4. New proposals for the design of stainless steel plate girders in fire

In this section, new fire design rules for stainless steel plate girders are proposed. The accuracy and reliability of the proposed fire design rules are also extensively verified against the results from nonlinear shell finite element modelling, taking into account a broad range of parameters affecting the structural response of stainless steel plate girders in fire.

4.1. Proposed design rules

Adopting the rotated stress field method [11–13] used for the room temperature design of stainless steel plate girders in EN 1993-1-4 [10], the following equation is recommended for the determination of the shear resistance $V_{b,Rd,\theta}$ of a stainless steel plate girder at temperature θ:

$$V_{b,Rd,\theta} = V_{bw,Rd,\theta} + V_{bf,Rd,\theta} \leq \frac{k_{2,\theta} f_{yw} h_w t_w}{\sqrt{3}\gamma_{M,fi}}, \tag{18}$$

where $k_{2,\theta}$ is the elevated temperature material strength reduction factor at 2% total strain and f_{yw} is the 0.2% proof strength of the web. In eq. (18), $V_{bw,Rd,\theta}$ is the web shear buckling resistance at temperature θ, $V_{bf,Rd,\theta}$ is the flange contribution at temperature θ, $\gamma_{M,fi}$ is the partial factor for resistance in fire conditions, h_w is the web height and t_w is the web thickness. The web shear buckling resistance $V_{bw,Rd,\theta}$ at temperature θ can be determined using the following expression:

$$V_{bw,Rd,\theta} = \frac{\chi_{w,\theta} k_{2,\theta} f_{yw} h_w t_w}{\sqrt{3}\gamma_{M,fi}}, \tag{19}$$

in which $\chi_{w,\theta}$ is the elevated temperature web shear buckling reduction factor. The flange contribution $V_{bf,Rd,\theta}$ at temperature θ is determined as:

$$V_{bf,Rd,\theta} = \left(\frac{b_f t_f^2 k_{2,\theta} f_{yf}}{c\gamma_{M,fi}}\right)\left[1 - \left(\frac{M_{Ed}}{M_{f,Rd,\theta}}\right)^2\right], \tag{20}$$

in which M_{Ed} is the applied bending moment, $M_{f,Rd,\theta}$ is the bending moment resistance of the cross-section determined considering the flanges only at temperature θ, b_f is the flange width, t_f is the flange thickness, $k_{2,\theta}$ is the elevated temperature material strength reduction factor at 2% total strain and f_{yf} is the room temperature 0.2% proof strength of the flanges. In eq. (20), the distance c specifies the location of the plastic hinges developing within the flanges. Through the same equation used in the room temperature design of stainless steel plate girders, c is determined as:

$$c = \left(0.17 + \frac{3.5 b_f t_f^2 f_{yf}}{t_w h_w^2 f_{yw}}\right) a \quad \text{with} \quad \frac{c}{a} \leq 0.65. \tag{21}$$

The elevated temperature shear buckling reduction factor $\chi_{w,\theta}$ is determined as shown in Table 5 where $\overline{\lambda}_{w,\theta}$ is the non-dimensional elevated temperature web slenderness calculated

Table 5: Elevated temperature shear buckling reduction factors $\chi_{w,\theta}$ for stainless steel plate girders with rigid and non-rigid end posts

	$\chi_{w,\theta}$ for rigid end post	$\chi_{w,\theta}$ for non-rigid end post
$\overline{\lambda}_{w,\theta} < 0.4$	1.0	1.0
$\overline{\lambda}_{w,\theta} \geq 0.4$	$0.9/(0.5 + \overline{\lambda}_{w,\theta})$	$0.8/(0.4 + \overline{\lambda}_{w,\theta})$

as:

$$\overline{\lambda}_{w,\theta} = \overline{\lambda}_w \xi_\theta = \sqrt{\frac{f_{yw}/\sqrt{3}}{\tau_{cr}}}\sqrt{\frac{k_{2,\theta}}{k_{E,\theta}}}, \tag{22}$$

where τ_{cr} is the elastic critical shear buckling stress of the plate girder which can be determined through the formulae provided in Annex A.3 of EN 1993-1-5 [50] and $\xi_\theta = \sqrt{k_{2,\theta}/k_{E,\theta}}$ is the elevated temperature strength-to-stiffness ratio reduction factor.

In line with EN 1993-1-4 [10] and EN 1993-1-5 [50], the following expression is recommended to consider the bending moment-shear interaction:

$$\overline{\eta}_1 + \left(1 - \frac{M_{f,Rd,\theta}}{M_{pl,Rd,\theta}}\right)(2\overline{\eta}_3 - 1)^2 \leq 1.0 \quad \text{for} \quad \overline{\eta}_1 \geq \frac{M_{f,Rd,\theta}}{M_{pl,Rd,\theta}}, \tag{23}$$

in which $M_{pl,Rd,\theta}$ is the design plastic resistance of the cross-section consisting of the effective area of the flanges and fully effective web irrespective of its section class at temperature θ. This study recommends performing the cross-section classification and the determination of

the effective widths of the flanges using the cross-section classification rules and effective width equations provided in Annex C of the upcoming version of the European structural steel fire design standard prEN 1993-1-2 [46], which are based on the recent proposals of Xing et al. [58, 59]. In eq. (23), $\overline{\eta}_1$ is an auxiliary coefficient calculated as

$$\overline{\eta}_1 = \frac{M_{Ed}}{M_{pl,Rd,\theta}}, \tag{24}$$

and $\overline{\eta}_3$ is also an auxiliary coefficient calculated using the following equation:

$$\overline{\eta}_3 = \frac{V_{Ed}}{V_{bw,Rd,\theta}}. \tag{25}$$

Note that in the application of the proposed design rules, the use of the material reduction factors $k_{2,\theta}$ and $k_{E,\theta}$ for stainless steel in fire recommended by [41] and adopted in Annex C of the upcoming version of the European structural steel fire design standard prEN 1993-1-2 [46] is recommended. Moreover, in addition to the shear design checks provided above, the bending moment M_{Ed} applied to a plate girder in fire should not exceed the elevated temperature bending moment resistance $M_{c,Rd,\theta}$ of the plate girder which can be determined using the fire design provisions for stainless steel sections provided in Annex C of prEN 1993-1-2 [46] as adopted from [58, 59], i.e. $M_{Ed} \leq M_{c,Rd,\theta}$.

Finally, it is worthwhile indicating that in the determination of the elevated temperature shear buckling reduction factor $\chi_{w,\theta}$, the use of the elevated temperature web slenderness $\overline{\lambda}_{w,\theta} = \overline{\lambda}_w \xi_\theta = \overline{\lambda}_w \sqrt{k_{2,\theta}/k_{E\theta}}$ given by eq. (22) in lieu of the room temperature web slenderness $\overline{\lambda}_w$ is recommended for the purpose of accounting for the differential erosions of the strength and stiffness of stainless steel at elevated temperatures, which is expected to result in more accurate assessment of the structural response of stainless steel plate girders in fire. In [58, 59], a similar approach was also adopted for the determination of the local buckling strengths of stainless steel plates and cross-sections in fire which is shown to result in accurate assessments of the local buckling response of stainless steel plates and cross-sections at elevated temperatures.

4.2. Accuracy assessment

In Fig. 11, the accuracy of the proposed design equations for austenitic and duplex stainless steel plate girders with rigid and non-rigid end posts in fire is shown for the web shear resistance predictions, where a wide range of parameters summarised in Table 3 are taken into account. Note that in Fig. 11, stainless steel plate girders subjected to a shear dominant failure mode (i.e. Case 1) are considered and the elevated temperature shear buckling reduction factors $\chi_{w,\theta,GMNIA}$ from the GMNIA are determined through eq. (13) with $M_{f,Rd,\theta}$ calculated using the cross-section classification approach and effective width equations for stainless steel sections provided in prEN 1993-1-2 [46] as adopted from [58, 59]. As can be seen from Fig. 11, the proposed fire design rules lead to safe web shear strength predictions for stainless steel plate girders in fire. Note that the conservative ultimate strength predictions of the proposed design rules are for stainless steel plate girders with

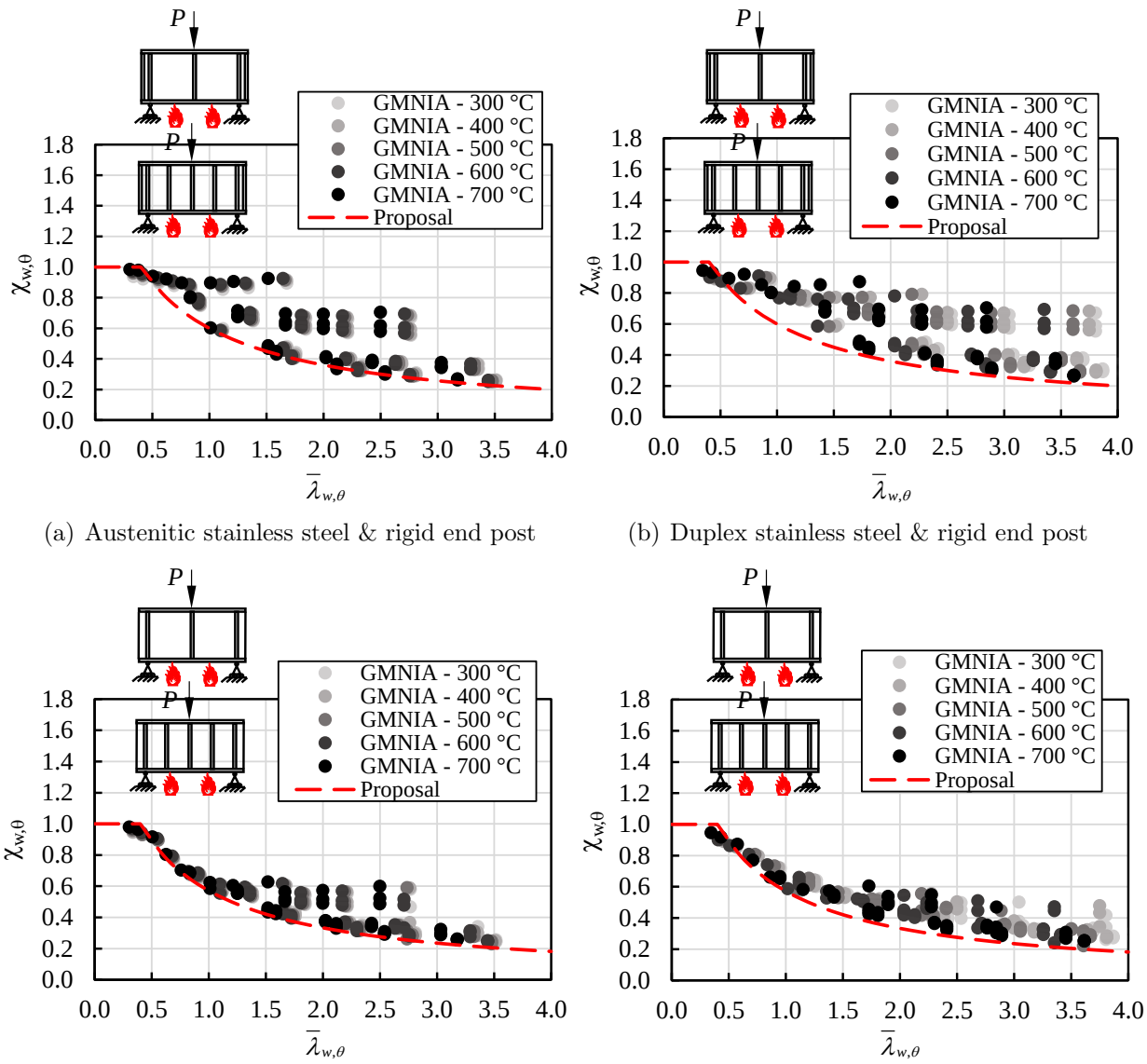

(a) Austenitic stainless steel & rigid end post

(b) Duplex stainless steel & rigid end post

(c) Austenitic stainless steel & non-rigid end post

(d) Duplex stainless steel & non-rigid end post

Figure 11: Accuracy of the proposed design approach for the fire design of stainless steel plate girders undergoing a shear dominant failure mode

rigid end posts and low unstiffened length a to web height h_w (i.e. a/h_w) ratios which exhibit significant post ultimate strengths; this type of conservative ultimate strength estimations were also observed in the design methods developed for the room temperature ultimate resistance predictions of stainless steel plate girders with low a/h_w ratios [5]. It may be possible to reduce this conservatism by making the elevated temperature shear buckling reduction factor $\chi_{w,\theta}$ a function of a/h_w for stainless steel plate girders with rigid end posts, though this (i) increases the complexity of the design method only for stainless steel plate girders with rigid end posts and (ii) is also not adopted in the room temperature design

methods for both carbon steel and stainless steel plate girders provided in EN 1993-1-5 [50] and EN 1993-1-4 [10] respectively. Thus, the elevated temperature shear buckling reduction factor $\chi_{w,\theta}$ equations provided in Table 5 for the design of stainless steel plate girders with rigid end posts in fire are not functions of a/h_w ratios for the sake of simplicity and compatibility with the existing room temperature design methods for carbon steel and stainless steel plate girders in EN 1993-1-5 [50] and EN 1993-1-4 [10]. Comparing Fig. 11 against Fig. 7, it is clear that the proposed fire design rules result in more accurate and safe assessment of the shear buckling response of stainless steel plate girders in fire relative to the EN 1993-1-4 [10] stainless steel plate girder design rules applied with the elevated temperature material properties of stainless steel.

The accuracy of the proposed design rules for stainless steel plate girders in fire is also shown in Fig. 12 for austenitic and duplex stainless steel plate girders in fire with rigid and non-rigid end posts which undergo (i) shear dominant failure modes (i.e. Case 1 failure modes) or (ii) bending dominant or combined bending and shear failure modes (i.e. Case 2 failure modes). Note that in the figure, the normalised moment-shear M-V interaction diagrams are created through eq. (23), where M-V int. (av.), M-V int. (max.) and M-V int. (min.) correspond to the average, maximum and minimum normalised moment-shear M-V interaction diagrams generated considering all the stainless steel plate girders taken into account in the numerical parametric studies which are set out in Table 3. As previously indicated, since the shapes of the normalised moment-shear M-V interaction diagrams depend on $V_{b,w,Rd,\theta}/V_{b,f,Rd,\theta}$ and $M_{f,Rd,\theta}/M_{pl,Rd,\theta}$ ratios, the normalised moment-shear M-V interaction diagrams are different for each considered stainless steel plate girder in the parametric studies and there is not a single curve that can be used for accuracy assessment. As can be seen from Fig. 12, the proposed fire design methods lead to safe ultimate resistance predictions for austenitic and duplex stainless steel plate girders with rigid and non-rigid end posts in fire which undergo either Case 1 or Case 2 failure modes.

In Fig. 13, the accuracy of the proposed design approach is also compared against that of EN 1993-1-4 [10] stainless steel plate girder design rules applied with the elevated temperature properties of stainless steel for austenitic and duplex stainless steel plate girders with rigid and non-rigid end posts in fire. Note that in Fig. 13, all the parameters taken into account in the numerical parametric studies summarised in Table 3 and both Case 1 and Case 2 failure modes are considered. Moreover, in the figure, ϕ corresponds to the radial angle in the normalised moment-shear M-V interaction diagrams as shown in Fig. 8 and $V_{Ed,GMNIA}$, $V_{Ed,prop}$ and $V_{Ed,EC3}$ correspond to the ultimate shear resistances determined through the GMNIA, proposed design approach and EN 1993-1-4 [10] applied with the elevated temperature material properties of stainless steel. As can be seen from Fig. 13, the proposed design approach leads to considerably more accurate and safe ultimate strength predictions relative to EN 1993-1-4 [10] applied with the elevated temperature material properties of stainless steel. A statistical appraisal of the accuracy of the proposed design method and that of EN 1993-1-4 [10] applied with the elevated temperature material properties of stainless steel is also set out in Table 6. In the table, N is the number of considered plate girders, ϵ is the ratio of the ultimate shear resistance obtained from the GMNIA $V_{Ed,GMNIA}$ to that determined through a design method $V_{Ed,prop}$ or $V_{Ed,EC3}$ ($\epsilon = V_{Ed,GMNIA}/V_{Ed,prop}$ in the ac-

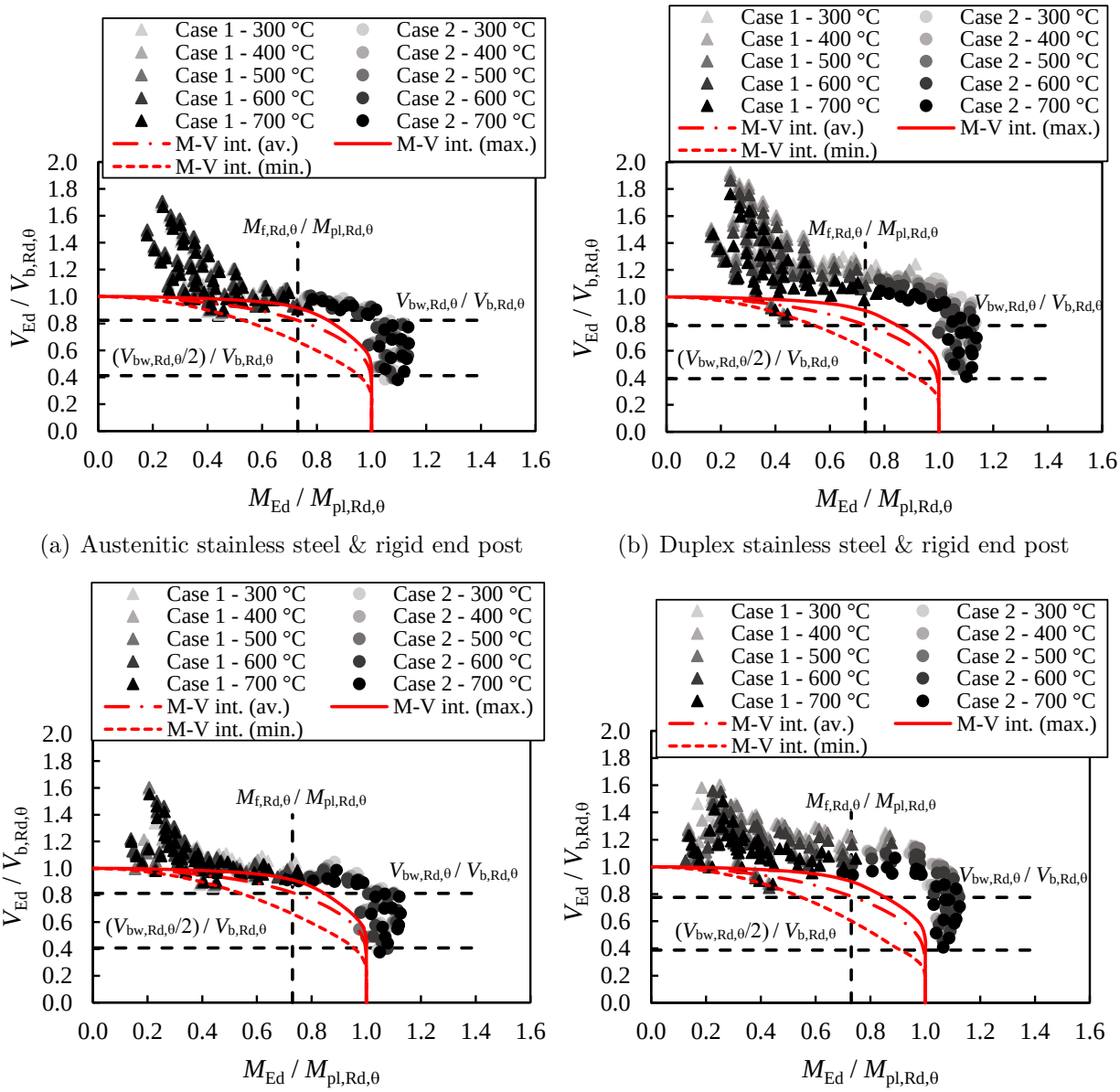

(a) Austenitic stainless steel & rigid end post

(b) Duplex stainless steel & rigid end post

(c) Austenitic stainless steel & non-rigid end post

(d) Duplex stainless steel & non-rigid end post

Figure 12: Normalised moment-shear interaction (M-V int.) diagram obtained from the proposed design approach and its accuracy against GMNIA for stainless steel plate girders in fire

curacy assessment of the proposed design rules and $\epsilon = V_{Ed,GMNIA}/V_{Ed,EC3}$ in the accuracy assessment of EN 1993-1-4 [10] applied with the elevated temperature material properties of stainless steel). Moreover, ϵ_{av}, ϵ_{COV}, ϵ_{max} and ϵ_{min} are the average, coefficient of variation, maximum and minimum of ϵ values for all the considered stainless steel plate girders. As can be seen from Table 6, the proposed design approach leads to considerably lower ϵ_{COV} ratios relative to EN 1993-1-4 [10] applied with the elevated temperature material properties of stainless steel which highlight the considerably higher accuracy and consistency of

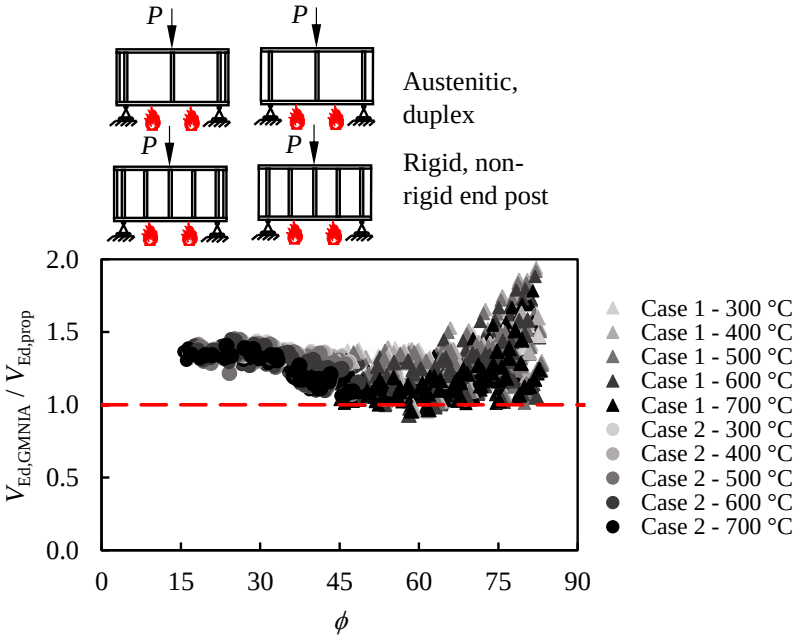

(a) Proposal

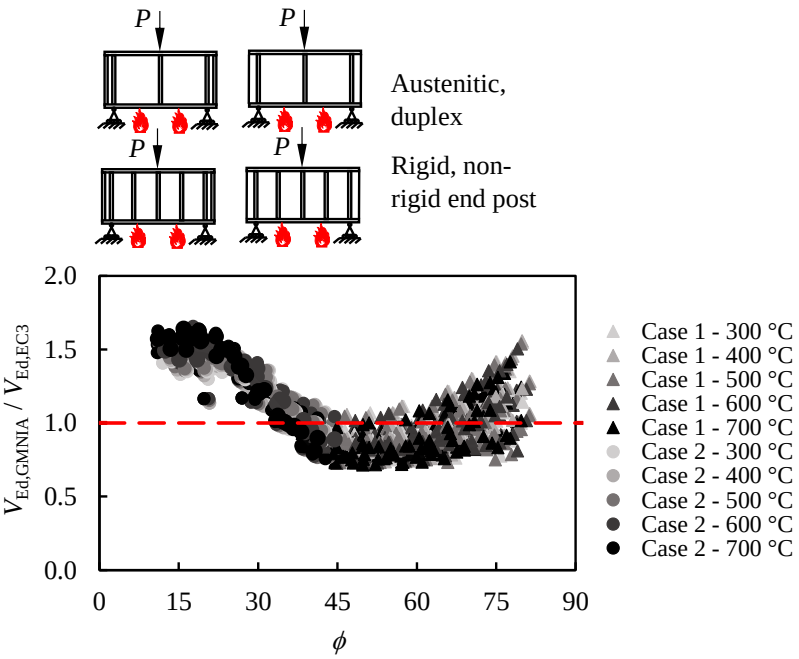

(b) EN 1993-1-4

Figure 13: Accuracy of the proposed design approach and EN 1993-1-4 applied with the elevated temperature material properties of stainless steel for stainless steel plate girders in fire

the proposed design rules. Comparison of the ϵ_{min} values of the proposed design approach against those of EN 1993-1-4 [10] applied with the elevated temperature material properties

Table 6: Accuracy assessment of the proposed fire design rules for stainless steel plate girders against the EN 1993-1-4 [10] stainless steel plate girder design rules applied with the elevated temperature material properties of stainless steel

		Proposal				EN 1993-1-4			
	N	ϵ_{av}	ϵ_{COV}	ϵ_{max}	ϵ_{min}	ϵ_{av}	ϵ_{COV}	ϵ_{max}	ϵ_{min}
Austenitic & rigid end post	350	1.24	0.132	1.73	0.95	1.07	0.227	1.63	0.73
Austenitic & non-rigid end post	350	1.18	0.106	1.62	0.95	1.01	0.256	1.66	0.71
Duplex & rigid end post	350	1.37	0.131	1.94	0.97	1.15	0.193	1.65	0.78
Duplex & non-rigid end post	350	1.28	0.094	1.63	0.93	1.05	0.223	1.64	0.76

of stainless steel also indicates that the proposed design approach leads to safe ultimate resistance predictions for austenitic and duplex stainless steel plate girders with rigid and non-rigid end posts in fire, while EN 1993-1-4 [10] stainless steel plate girder design rules applied with the elevated temperature material properties of stainless steel can lead to quite unsafe resistance predictions.

4.3. Anisothermal analyses of stainless steel plate girders and further accuracy assessment of the proposed fire design approach

As previously indicated, an isothermal analysis approach was adopted in the GMNIA of the finite element models in this study where (i) first, the temperatures of the stainless steel plate girders were uniformly increased up to certain elevated temperature levels θ which resulted in the development of thermal strains and the modification of the material response and (ii) then, the finite element models were loaded up to failure which provided the ultimate load carrying capacities of the stainless steel plate girders at certain elevated temperature levels θ. It should be emphasised that the described isothermal analysis approach adopted in the finite element simulations in this paper (i) provides reliable and controllable ultimate resistance estimations at the designated elevated temperature levels θ and (ii) has been utilised in numerous previous research studies on the behaviour of steel structures in fire [55, 60–68]. In these studies [55, 60–68], using the benchmark results from the same isothermal analyses of the finite element models, fire design methods for structural steel elements were derived or assessed; some of the fire design methods developed in these studies [60, 63, 64] have been incorporated into EN 1993-1-2 [9] and its upcoming version prEN 1993-1-2 [46]. Reis et al. [53–55] also adopted the same isothermal analysis approach used in this study in the numerical analyses of the finite element models whereby benchmark ultimate resistances of carbon steel plate girders at designated elevated temperature levels were derived and used in the development of a fire design method for carbon steel plate girders.

For the purpose of assessing the adopted isothermal analysis technique, the finite element models of austenitic and duplex stainless steel plate girders were also analysed using an

anisothermal analysis approach which is also referred to as the transient analysis technique in the literature. In the anisothermal analysis approach, firstly, the heat transfer analyses of the finite element models of the stainless plate girders were carried out using the DS4 heat transfer shell element of Abaqus [33] where the finite element models were subjected to the ISO 834 standard fire [69]; the finite element models were exposed to fire on all four sides. In accordance with EN 1993-1-2 [9], the heat transfer coefficient α_c and emissivity ϵ_m were taken as 25 W/m^{2}K and 0.4, respectively (i.e. α_c =25 W/m^{2}K and ϵ_m=0.4). Following the heat transfer analyses, the mechanical analyses of the finite element models were performed where (i) first, the residual stresses were applied to the finite element models, (ii) then, the loading was applied to the finite element models at room temperature and (iii) finally, the finite element models were heated up to failure adopting the temperature development histories obtained from the priori heat transfer analyses while keeping the applied loading constant. Note that in accordance with Gardner and Ng [70] where it was shown that the shadow effects generally have small influence for stainless steel I-section elements, the shadow effects were conservatively not included in the heat transfer analyses. Examples of the temperature development within the web and flange plates of austenitic stainless steel plate girders with the cross-sections of I-600×200×10×15, I-600×200×6×15 and I-600×200×4×15 and the web panel aspect ratio a/h_w of 1.0 are illustrated in Fig. 14. Fig. 15 also shows the temperatures of the components of the finite element model of an austenitic stainless steel plate girder with the cross-section of I-600×200×6×15 and the web panel aspect ratio of 1.0 (i.e. $a/h_w = 1.0$) after the model was subjected to 5, 15, 25 and 50 min of ISO 834 standard fire in a heat transfer analysis. As can be seen in Figs. 14 and 15, the webs of the stainless steel plate girders are subjected to the highest rates of temperature increases and thus, the highest rates of strength and stiffness reductions. Considering that stainless steel plate girders primarily resist the applied shear loads by means of their webs, the adoption of a uniform temperature increase with an isothermal analysis approach where the finite element model of a stainless steel plate girder is uniformly heated to a certain elevated temperature level θ and then loaded up to failure is expected to furnish a safe and conservative ultimate resistance prediction for a stainless steel plate girder at that particular elevated temperature level θ.

In Fig. 16, the ultimate shear force and bending moment resistances obtained from the anisothermal and isothermal analyses are illustrated for austenitic and duplex stainless steel plate girders with rigid and non-rigid end posts and the web panel aspect ratios a/h_w of 1.0, 2.0 and 3.0. In the figure, the results for the austenitic and duplex stainless steel plate girders with the cross-section of I-600×200×t_w×15 where the web thickness t_w ranged between 2 mm and 10 mm are illustrated (i.e. 2 mm $\leq t_w \leq$ 10 mm), enabling the consideration of various elevated temperature web slendernesses $\overline{\lambda}_{w,\theta}$. In total, 252 austenitic and duplex stainless steel plate girders were analysed through the anisothermal analysis technique. The accuracy of the proposed fire design approach is also displayed in Fig. 16. In the figure, the ultimate shear force $V_{Ed,GMNIA}$ and bending moment $M_{Ed,GMNIA}$ resistances determined through the anisothermal and isothermal analyses of the stainless steel plate girders are normalised by the elevated temperature shear resistances $V_{b,Rd,\theta}$ and the plastic bending moment resistances $M_{pl,Rd,\theta}$ (with the effective areas of the flanges and fully effective webs)

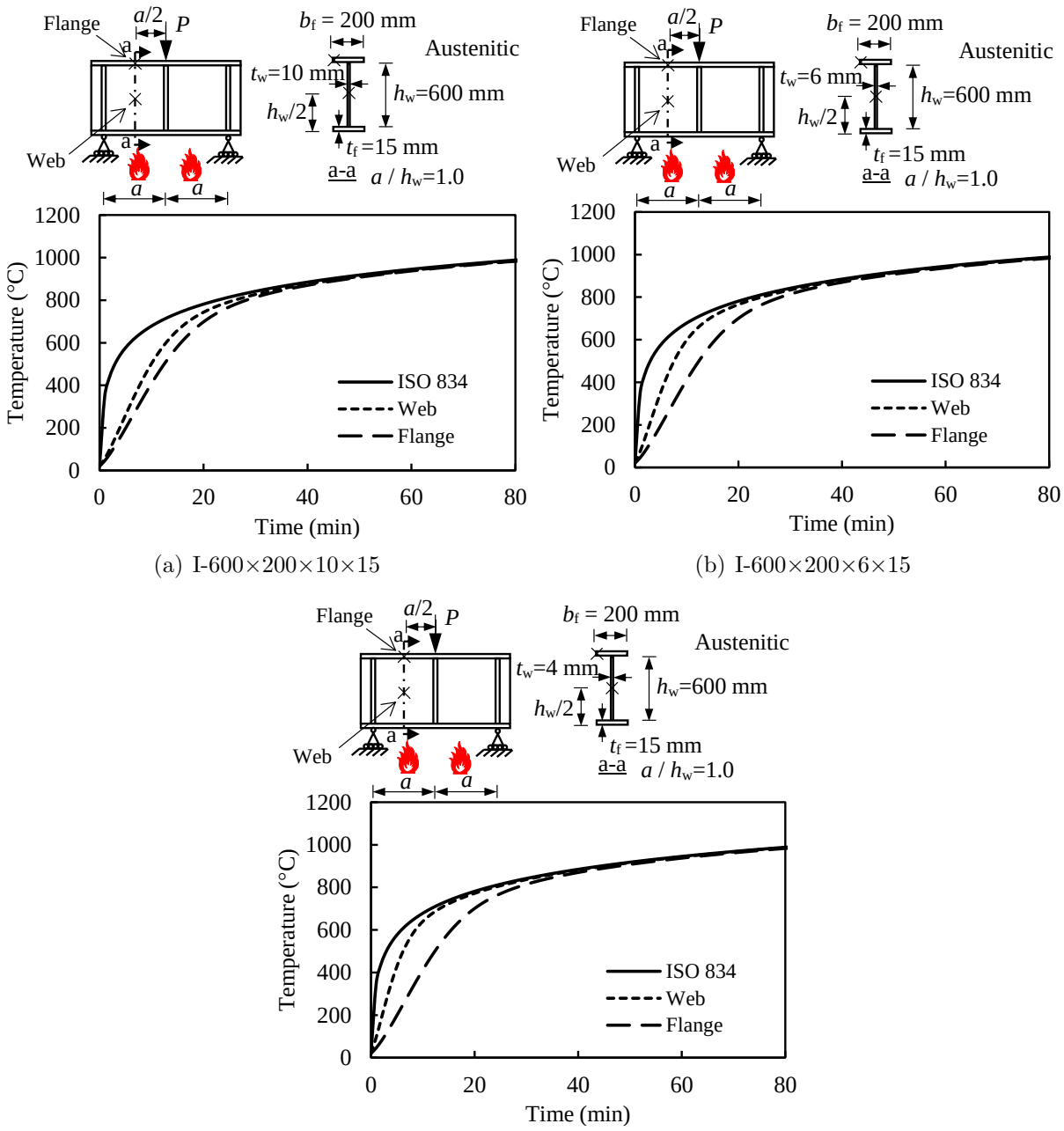

(a) I-600×200×10×15

(b) I-600×200×6×15

(c) I-600×200×4×15

Figure 14: Comparison of the web and flange plate temperatures for austenitic stainless steel plate girders subjected to ISO 834 heating with non-rigid ends posts and web panel aspect ratio a/h_w of 1.0

determined through the proposed fire design approach in line with the interaction equation given by eq. (12). It should be noted that in the anisothermal analyses, the stainless steel plate girders were (i) first subjected to the loading P at room temperature which led to the internal shear forces $V_{Ed,GMNIA}$ that ranged from 15% to 75% of the room temperature

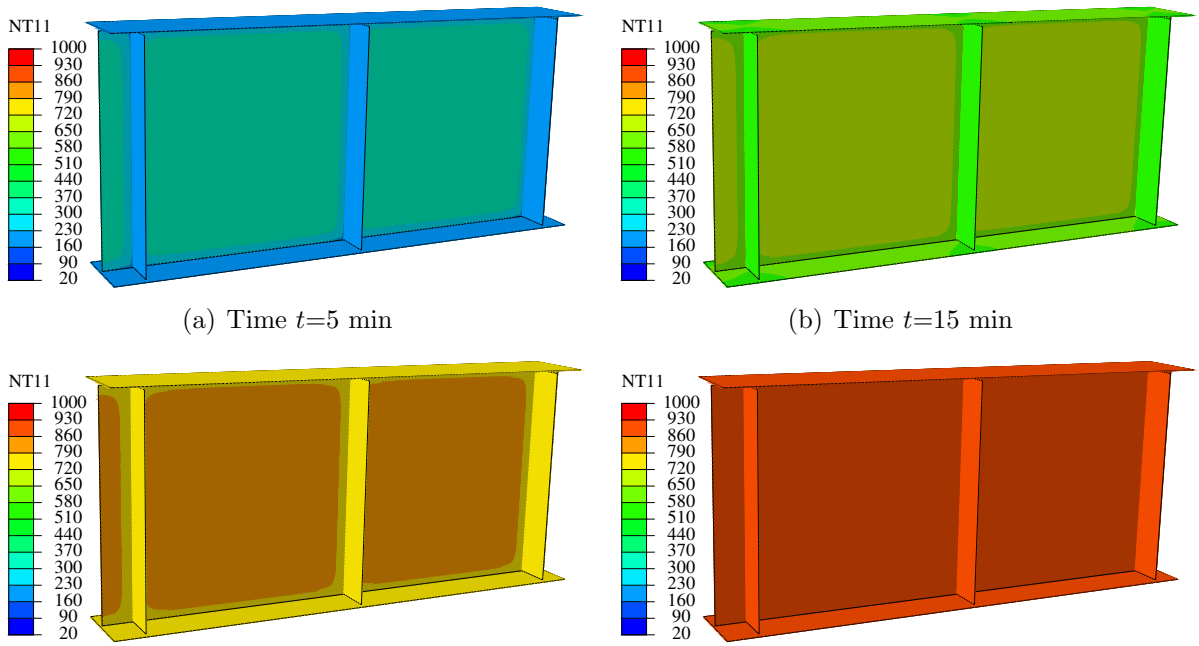

(a) Time t=5 min

(b) Time t=15 min

(c) Time t=25 min

(d) Time t=50 min

Figure 15: Temperatures within the components of an austenitic stainless steel plate girder with a web panel aspect ratio a/h_w of 1.0 and cross-section of I-600×200×6×15 after being subjected to t=5, 15, 25 and 50 min of ISO 834 standard fire

plastic web plate shear resistances (i.e. $V_{Ed,GMNIA} = 0.15h_w t_w f_{yw}/\sqrt{3} - 0.75h_w t_w f_{yw}/\sqrt{3}$) specified considering the ultimate values of the applied loads P determined through the isothermal analyses at 300 °C, 500 °C and 700 °C and (ii) then, heated up to failure using the temperature development histories from the priori heat transfer analyses. The critical temperatures θ_{cr} at which the plate girders could no longer withstand the applied loading were taken as the critical temperatures within the webs $\theta_{cr,w}$ in the anisothermal analyses (i.e. $\theta_{cr} = \theta_{cr,w}$). In the proposed method, the elevated temperature shear resistances $V_{b,Rd,\theta}$ and the plastic bending moment resistances $M_{pl,Rd,\theta}$ (with the effective areas of the flanges and fully effective webs) are determined assuming a uniform critical temperature distribution through the cross-section of a stainless steel plate girder.

As can be seen from Fig. 16, the proposed fire design approach leads to safe and accurate resistance predictions for the austenitic and duplex stainless steel plate girders analysed through the both anisothermal and isothermal analysis techniques. Fig. 16 shows that in some cases, the anisothermal analyses of the stainless steel plate girders lead to higher ultimate resistance predictions relative to those determined through the isothermal analyses; the anisothermal analysis predictions are higher particularly for the stainless steel plate girders undergoing the Case 2 failure modes (i.e. bending dominant and combined bending and shear failure modes). This is due to the lower temperature development rates in the flange plates relative to those in the web plates within the stainless steel plate girders which were taken into account in the anisothermal analyses of the finite element models but

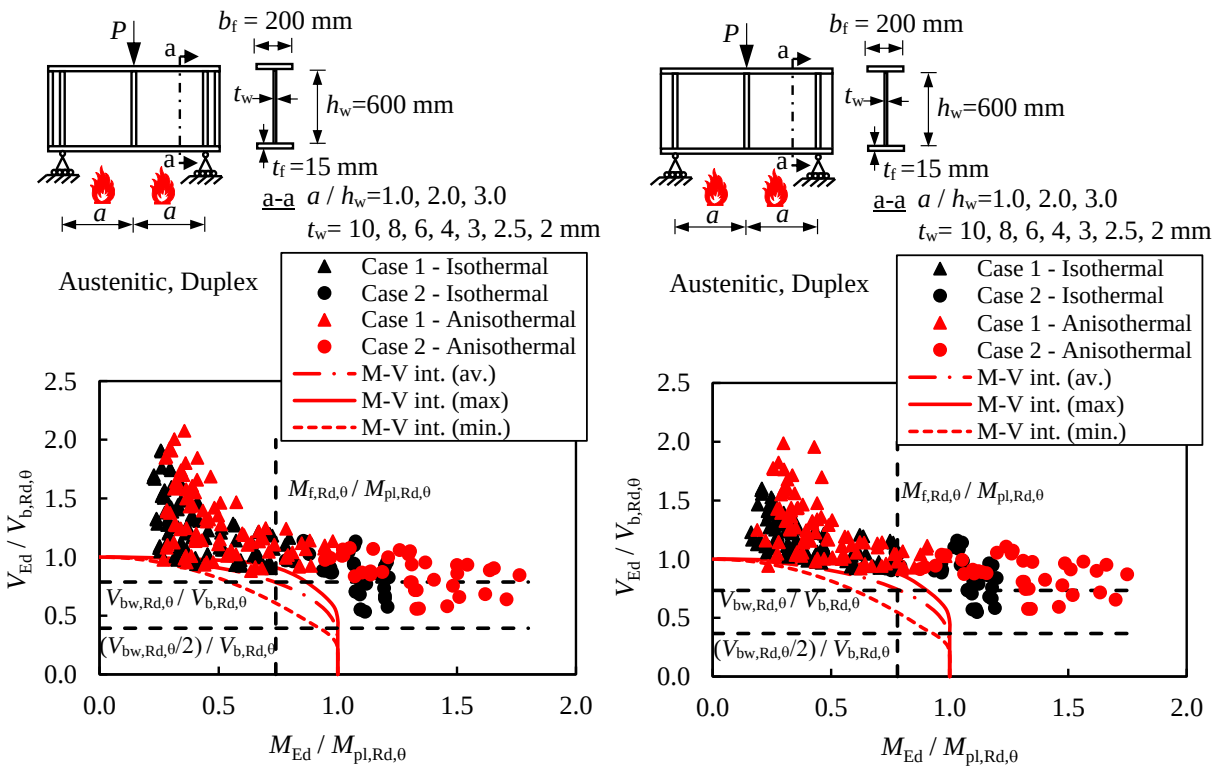

(a) Austenitic and duplex & rigid end post (b) Austenitic and duplex & non-rigid end post

Figure 16: Comparison of the ultimate shear force and bending moment resistances of austenitic and duplex stainless steel plate girders determined using the isothermal and anisothermal analysis methods in the GMNIA of the finite element models and accuracy of the proposed fire design approach

disregarded in the isothermal analyses of the finite element models owing to the uniform temperature assumption within the cross-sections. It should be emphasised though that the proposed fire design approach leads to safe ultimate resistance predictions when the ultimate resistances determined through the both analysis techniques are considered.

Comparison of the web shear buckling resistance predictions $V_{bw,Rd,\theta}$ determined by means of the anisothermal and isothermal analysis techniques is also shown in Fig. 17 for austenitic and duplex stainless steel plate girders with various elevated temperature web slendernesses $\overline{\lambda}_{w,\theta}$, rigid and non-rigid end posts and the web panel aspect ratios a/h_w of 1.0, 2.0 and 3.0. The numerical web shear buckling reduction factor $\chi_{w,\theta,GMNIA}$ from an anisothermal analysis was determined through eq. (13) using (i) the critical web temperature θ_{cr} at which the plate girder fails and (ii) the applied shear $V_{Ed,GMNIA}$ and bending moments $M_{Ed,GMNIA}$ to the finite element model which remained constant throughout the heating part of the anisothermal analysis; c and $M_{f,Rd,\theta}$ values determined according to the proposed fire design method were also utilised in eq. (13) for the determination of $\chi_{w,\theta,GMNIA}$. The numerical web shear buckling reduction factors $\chi_{w,\theta,GMNIA}$ from the isothermal analyses of the stainless steel plate girders analysed at 300 °C, 500 °C and 700 °C and the web shear buckling reduction factors $\chi_{w,\theta}$ determined using the proposed fire design approach by means

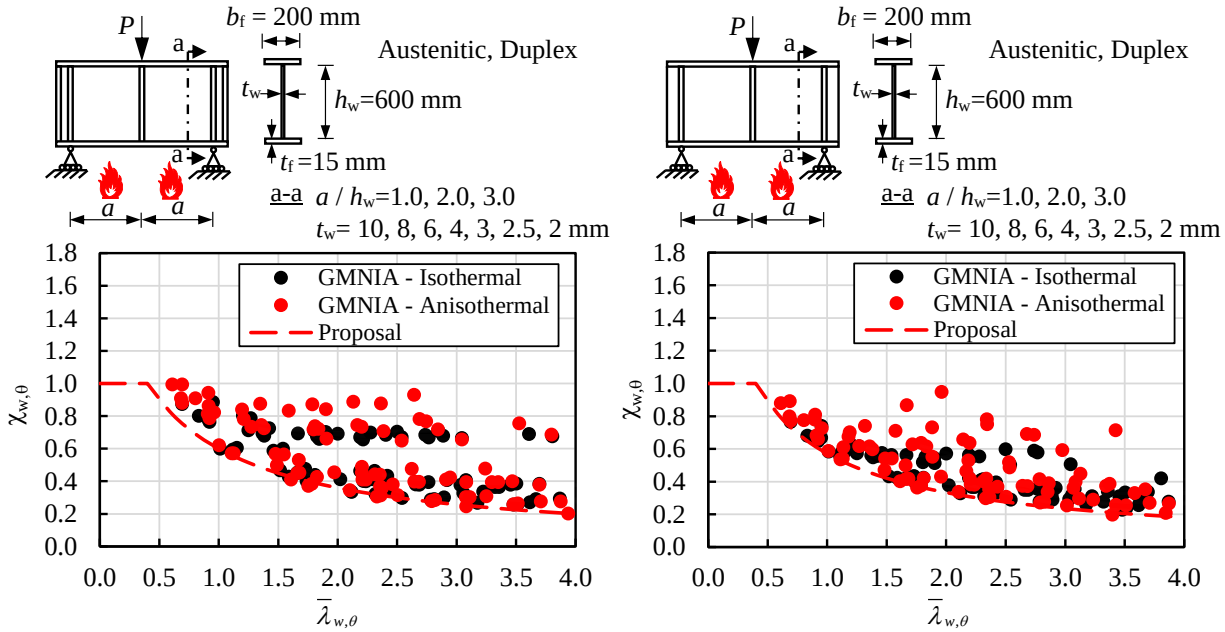

(a) Austenitic and duplex & rigid end post

(b) Austenitic and duplex & non-rigid end post

Figure 17: Comparison of the web shear buckling resistances of austenitic and duplex stainless steel plate girders determined using the isothermal and anisothermal analysis methods in the GMNIA of the finite element models and accuracy of the proposed fire design approach

of Table 5 are also shown in Fig. 17. As can be seen from Fig. 17, the numerical web shear buckling reduction factors $\chi_{w,\theta,GMNIA}$ determined through the anisothermal and isothermal analyses of the finite element models are not significantly different in a high number of cases owing to the highest temperature development rates observed in the web plates within the heating part of the anisothermal analyses and the proposed fire design approach furnishes safe web shear buckling resistance predictions on the basis of the results determined through the both anisothermal and isothermal analysis approaches.

The findings of this section indicate that both the isothermal and the anisothermal analysis techniques could be utilised for the assessment of the behaviour of stainless steel plate girders in fire and the proposed fire design approach leads to safe estimations of the structural response at elevated temperatures when the results from the both analysis approaches are considered. It should also be noted that the proposed fire design method could be readily modified to provide higher ultimate resistance predictions for stainless steel plate girders subjected to non-uniform temperature developments along their lengths and/or through their cross-section depths by means of modification factors applied to the ultimate resistance predictions; this will be explored in future research by investigating different temperature development scenarios within stainless steel plate girders.

4.4. Reliability assessment

The reliability of the proposed design approach for stainless steel plate girders in fire is assessed in this section through the three reliability criteria put forward by Kruppa [71] for

the fire design methods of steel structures, using the benchmark ultimate resistance predictions from the isothermal analyses of the finite element models. Criterion 1 of Kruppa [71] requires that none of the ultimate shear strength predictions determined through a design method $V_{Ed,method}$ (i.e. either the proposed design rules $V_{Ed,method} = V_{Ed,prop}$ or EN 1993-1-4 [10] applied with the elevated temperature material properties of stainless steel $V_{Ed,method} = V_{Ed,EC3}$) should be more than 15% greater than those determined by the FE $V_{Ed,GMNIA}$ (i.e. $(V_{Ed,method} - V_{Ed,GMNIA})/V_{Ed,GMNIA} \leq 1.15$). Criterion 2 of [71] requires less than 20% of the design predictions to be on the unsafe side, i.e. $num(V_{Ed,method} > V_{Ed,GMNIA})/num(V_{Ed,method}) \leq$20%. Finally, Criterion 3 of Kruppa[71] requires that the average of the ultimate resistance estimations of a design method should be on the safe side, i.e. $\overline{X}[(V_{Ed,method} - V_{Ed,GMNIA})\ /V_{Ed,GMNIA}] \leq 0\%$. Adopting the three reliability assessment criteria of Kruppa [71], the reliability assessment of the proposed rules for the design of stainless steel plate girders in fire and that of EN 1993-1-4 [10] stainless steel plate girder design rules applied with the elevated temperature material properties of stainless steel is shown in Table 7. In the table, the percentage of the plate girders for which the overesti-

Table 7: Reliability assessment of the proposed fire design rules for stainless steel plate girders and the EN 1993-1-4 [10] stainless steel plate girder design rules applied with the elevated temperature material properties of stainless steel

	Proposal			EN 1993-1-4		
	Criterion 1	Criterion 2	Criterion 3	Criterion 1	Criterion 2	Criterion 3
Austenitic & rigid end post	0.00	3.71	-17.71	27.43*	46.00*	-2.13
Austenitic & non-rigid end post	0.00	2.86	-14.67	46.57*	63.14*	5.03*
Duplex & rigid end post	0.00	1.43	-25.70	8.86*	32.00*	-9.87
Duplex & non-rigid end post	0.00	2.00	-21.41	22.57*	59.14*	-0.27

mations of the ultimate strengths exceeded 15% of those determined from the GMNIA is illustrated under Criterion 1, the percentage of the plate girders where the ultimate strengths are overestimated is shown under Criterion 2 and the average percentage of the differences between the design and finite element ultimate strength estimations are illustrated under Criterion 3. The violated criteria are specified with *. As can be seen from Table 7, the proposed fire design rules for stainless steel plate girders satisfy the three reliability criteria of Kruppa [71] in all the considered cases while the EN 1993-1-4 [10] stainless steel plate girder design rules applied with the elevated temperature material properties of stainless steel violate them in a high number of cases, indicating that the proposed design approach leads to a reliable assessment of the behaviour of stainless steel plate girders in fire.

5. Conclusions

In this paper, the structural response and design of stainless steel plate girders in fire have been explored. Shell finite element models of stainless steel plates girders capable of mimicking their behaviour in fire were created. The accuracy of the created finite element models was validated against the results from physical experiments on stainless steel plate girders at room temperature and carbon steel plate girders in fire. Comprehensive numerical parametric studies were performed to generate extensive benchmark structural performance data for stainless steel plate girders at elevated temperatures, taking into account austenitic and duplex stainless steel grades, various web slendernesses, rigid and non-rigid end posts, different unstiffened length to web height ratios and different elevated temperature levels. Due to the absence of specific fire design rules for stainless steel plate girders in the European structural steel fire design standard EN 1993-1-2 [9], the accuracy of the room temperature stainless steel plate girder design rules provided in the European structural stainless steel design standard EN 1993-1-4 [10] which were applied with the elevated temperature material properties of stainless steel was investigated. It was observed that the EN 1993-1-4 [10] stainless steel plate girder design rules applied with the elevated temperature material properties of stainless steel lead to rather inaccurate ultimate resistance predictions of stainless steel plate girders in fire, which can be quite unsafe in some instances. With the aim of accurately estimating the structural response of stainless steel plate girders at elevated temperatures, new fire design rules for stainless steel plate girders have been put forward. It was shown that the proposed fire design rules lead to safe ultimate resistance predictions for stainless steel plate girders in fire. The reliability of the proposed stainless steel plate girder fire design rules was also verified against the three reliability criteria of Kruppa [71] proposed for the reliability assessment of fire design methods for steel structures. In this study, the behaviour of stainless steel plate girders was investigated numerically. Future research should focus on fire experiments on stainless steel plate girders whose results could complement the findings of this research.

It should be noted that Annex C of the upcoming version of the European structural steel fire design standard prEN 1993-1-2 [46] involves a series of new fire design rules for stainless steel structural members based on the research performed by Kucukler et al. [57] and Xing et al. [58, 59]. The stainless steel plate girder fire design rules presented in this paper are compatible with the format of the new structural stainless steel fire design rules included in prEN 1993-1-2 [46], thereby extending these design rules to cover the fire design of stainless steel plate girders.

Acknowledgements

The research presented in this paper is funded by the Engineering and Physical Sciences Research Council (EPSRC) of the UK under the grant number EP/V034405/1. The author gratefully acknowledges the financial support provided by the EPSRC for the research presented in this paper.

References

[1] Olsson, A.. Stainless steel plasticity: Material modelling and structural applications. Ph.D. thesis; Luleå University of Technology; 2001.

[2] Estrada, I., Real, E., Mirambell, E.. General behaviour and effect of rigid and non-rigid end post in stainless steel plate girders loaded in shear. Part I: Experimental study. Journal of Constructional Steel Research 2007;63(7):970–984.

[3] Real, E., Mirambell, E., Estrada, I.. Shear response of stainless steel plate girders. Engineering Structures 2007;29(7):1626–1640.

[4] Saliba, N., Gardner, L.. Experimental study of the shear response of lean duplex stainless steel plate girders. Engineering Structures 2013;46:375–391.

[5] Saliba, N., Real, E., Gardner, L.. Shear design recommendations for stainless steel plate girders. Engineering Structures 2014;59:220–228.

[6] Chen, X., Yuan, H., Du, X., Zhao, Y., Ye, J., Yang, L.. Shear buckling behaviour of welded stainless steel plate girders with transverse stiffeners. Thin-Walled Structures 2018;122:529–544.

[7] Yuan, H., Chen, X., Theofanous, M., Wu, Y., Cao, T., Du, X.. Shear behaviour and design of diagonally stiffened stainless steel plate girders. Journal of Constructional Steel Research 2019;153:588–602.

[8] Fortan, M., Ferraz, G., Lauwens, K., Molkens, T., Rossi, B.. Shear buckling of stainless steel plate girders with non-rigid end posts. Journal of Constructional Steel Research 2020;172:106211.

[9] EN 1993-1-2, Eurocode 3 Design of steel structures-Part 1-2: General rules – Structural fire design. European Committee for Standardization (CEN), Brussels; 2005.

[10] EN 1993-1-4, Eurocode 3 Design of steel structures-Part 1-2: General rules – Supplementary rules for stainless steel. European Committee for Standardization (CEN), Brussels; 2005.

[11] Höglund, T.. Behaviour and strength of the web of thin plate I-girders, Bulletin No. 94, the Division of Building Statics and Structural Engineering, The Royal Institute of Technology, Stockholm, Sweden. 1971.

[12] Höglund, T.. Design of thin plate I-girders in shear and bending with special reference to web buckling, Bulletin No. 94, the Division of Building Statics and Structural Engineering, The Royal Institute of Technology, Stockholm, Sweden. 1973.

[13] Höglund, T.. Shear buckling resistance of steel and aluminium plate girders. Thin-Walled structures 1997;29(1-4):13–30.

[14] Gardner, L., Baddoo, N.. Fire testing and design of stainless steel structures. Journal of Constructional Steel Research 2006;62(6):532–543.

[15] Uppfeldt, B., Outinen, T.A., Veljkovic, M.. A design model for stainless steel box columns in fire. Journal of Constructional Steel Research 2008;64(11):1294–1301.

[16] Tondini, N., Rossi, B., Franssen, J.M.. Experimental investigation on ferritic stainless steel columns in fire. Fire Safety Journal 2013;62:238–248.

[17] Fan, S., Ding, X., Sun, W., Zhang, L., Liu, M.. Experimental investigation on fire resistance of stainless steel columns with square hollow section. Thin-Walled Structures 2016;98:196–211.

[18] Fan, S., Li, Y., Li, Z., Liu, M., Han, Y.. Experimental investigation of fire resistance of axially compressed stainless steel columns with constraints. Thin-Walled Structures 2017;120:46–59.

[19] Fan, S., Liu, M., Sun, W., Guo, Y., Han, Y.L.. Experimental investigation of eccentrically compressed stainless steel columns with constraints in fire. Fire Safety Journal 2018;99:49–62.

[20] Ding, R., Fan, S., Chen, G., Li, C., Du, E., Liu, C.. Fire resistance design method for restrained stainless steel h-section columns under axial compression. Fire Safety Journal 2019;108:102837.

[21] Liu, M., Fan, S., Ding, R., Chen, G., Du, E., Wang, K.. Experimental investigation on the fire resistance of restrained stainless steel h-section columns. Journal of Constructional Steel Research 2019;163:105770.

[22] Liu, M., Duan, S., Wu, Y., Fan, S., Xu, Q.. Fire resistance design of austenitic SUS316 stainless columns subjected to axial compression. Journal of Constructional Steel Research 2022;198:107540.

[23] Xing, Z., Zhao, O., Kucukler, M., Gardner, L.. Testing of stainless steel i-section columns in fire. Engineering Structures 2021;227:111320.
[24] Xing, Z., Zhao, O., Kucukler, M., Gardner, L.. Fire testing of austenitic stainless steel I-section beam–columns. Thin-Walled Structures 2021;164:107916.
[25] Xing, Z., Zhao, O., Kucukler, M., Gardner, L.. Fire testing and design of slender stainless steel I-sections in weak-axis flexure. Thin-Walled Structures 2022;171:108682.
[26] Fan, S., He, B., Xia, X., Gui, H., Liu, M.. Fire resistance of stainless steel beams with rectangular hollow section: Experimental investigation. Fire safety journal 2016;81:17–31.
[27] Fan, S., Du, L., Li, S., Zhang, L., Shi, K.. Fire-resistance of rhs stainless steel beams with three faces exposed to fire. Journal of Constructional Steel Research 2019;152:284–295.
[28] He, A., Liang, Y., Zhao, O.. Experimental and numerical studies of austenitic stainless steel CHS stub columns after exposed to elevated temperatures. Journal of Constructional Steel Research 2019;154:293–305.
[29] He, A., Li, H.T., Lan, X., Liang, Y., Zhao, O.. Flexural buckling behaviour and residual strengths of stainless steel CHS columns after exposure to fire. Thin-Walled Structures 2020;152:106715.
[30] He, A., Sun, Y., Wu, N., Zhao, O.. Testing, simulation and design of eccentrically loaded austenitic stainless steel CHS stub columns after exposure to elevated temperatures. Thin-Walled Structures 2021;164:107885.
[31] Lan, X., Li, S., Zhao, O.. Local buckling of hot-rolled stainless steel channel section stub columns after exposure to fire. Journal of Constructional Steel Research 2021;187:106950.
[32] Reis, A., Lopes, N., Real, E., Vila Real, P.. Stainless steel plate girders subjected to shear buckling at normal and elevated temperatures. Fire technology 2017;53(2):815–843.
[33] Abaqus 2018 Reference Manual. Simulia, Dassault Systemes; 2018.
[34] Kucukler, M.. Lateral instability of steel beams in fire: Behaviour, numerical modelling and design. Journal of Constructional Steel Research 2020;170:106095.
[35] Kucukler, M.. Compressive resistance of high-strength and normal-strength steel CHS members at elevated temperatures. Thin-Walled Structures 2020;152:106753.
[36] Kucukler, M., Gardner, L.. In-plane structural response and design of duplex and ferritic stainless steel welded I-section beam–columns. Engineering Structures 2021;247:113136.
[37] Boissonnade, N., Somja, H.. Influence of imperfections in FEM modeling of lateral torsional buckling. Proceedings of the Structural Stability Research Council Annual Stability Conference; 2012; 18–21.
[38] Taras, A., Greiner, R.. New design curves for lateral–torsional buckling—proposal based on a consistent derivation. Journal of Constructional Steel Research 2010;66(5):648–663.
[39] Kucukler, M., Gardner, L., Macorini, L.. Lateral–torsional buckling assessment of steel beams through a stiffness reduction method. Journal of Constructional Steel Research 2015;109:87–100.
[40] Saliba, N.G., Gardner, L.. Deformation-based design of stainless steel cross-sections in shear. Thin-Walled Structures 2018;123:324–332.
[41] Structural Stainless Steel Design Manual, Fourth Edition. Steel Construction Institute (SCI); 2017.
[42] Gardner, L., Insausti, A., Ng, K., Ashraf, M.. Elevated temperature material properties of stainless steel alloys. Journal of Constructional Steel Research 2010;66(5):634–647.
[43] Ramberg, W., Osgood, W.R.. Description of stress-strain curves by three parameters. Technical note no. 902, National Advisory Committee on Aeronautics (NACA); 1943.
[44] Afshan, S., Zhao, O., Gardner, L.. Standardised material properties for numerical parametric studies of stainless steel structures and buckling curves for tubular columns. Journal of Constructional Steel Research 2019;152:2–11.
[45] Liang, Y., Manninen, T., Zhao, O., Walport, F., Gardner, L.. Elevated temperature material properties of a new high-chromium austenitic stainless steel. Journal of Constructional Steel Research 2019;152:261–273.
[46] prEN 1993-1-2, Final Draft of Eurocode 3 Design of steel structures-Part 1-2: General rules - Structural fire design. European Committee for Standardization (CEN), Brussels; 2020.
[47] Yuan, H., Wang, Y., Shi, Y., Gardner, L.. Residual stress distributions in welded stainless steel

sections. Thin-Walled Structures 2014;79:38–51.
[48] Kucukler, M.. Local stability of normal and high strength steel plates at elevated temperatures. Engineering Structures 2021;243:112528.
[49] EN 1990-2, Execution of Steel Structures and Aluminium Structures-Part 2: Technical Requirements for Steel Structures. European Committee for Standardization (CEN), Brussels; 2008.
[50] EN 1993-1-5, Eurocode 3 Design of steel structures-Part 1-5: Plated structural elements. European Committee for Standardization (CEN), Brussels; 2005.
[51] Chacon, R., Mirambell, E., Real, E.. Influence of flange strength on transversally stiffened girders subjected to patch loading. Journal of Constructional Steel Research 2014;97:39–47.
[52] Chacon, R., Mirambell, E., Real, E.. Influence of designer-assumed initial conditions on the numerical modelling of steel plate girders subjected to patch loading. Thin-Walled Structures 2009;47(4):391–402.
[53] Reis, A., Lopes, N., Vila Real, P.. Numerical study of steel plate girders under shear loading at elevated temperatures. Journal of Constructional Steel Research 2016;117:1–12.
[54] Reis, A., Lopes, N., Vila Real, P.. Shear–bending interaction in steel plate girders subjected to elevated temperatures. Thin-Walled Structures 2016;104:34–43.
[55] Reis, A., Lopes, N., Vila Real, P.. Ultimate shear strength of steel plate girders at normal and fire conditions. Thin-Walled Structures 2019;137:318–330.
[56] Vimonsatit, V., Tan, K.H., Qian, Z.H.. Testing of plate girder web panel loaded in shear at elevated temperature. Journal of Structural Engineering, ASCE 2007;133(6):815–824.
[57] Kucukler, M., Xing, Z., Gardner, L.. Behaviour and design of stainless steel I-section columns in fire. Journal of Constructional Steel Research 2020;165:105890.
[58] Xing, Z., Kucukler, M., Gardner, L.. Local buckling of stainless steel I-sections in fire: Finite element modelling and design. Thin-Walled Structures 2021;161:107486.
[59] Xing, Z., Kucukler, M., Gardner, L.. Local buckling of stainless steel plates in fire. Thin-Walled Structures 2020;148:106570.
[60] Vila Real, P., Piloto, P., Franssen, J.M.. A new proposal of a simple model for the lateral-torsional buckling of unrestrained steel I-beams in case of fire: Experimental and numerical validation. Journal of Constructional Steel Research 2003;59(2):179–199.
[61] Lopes, N., Real, P.V., da Silva, L.S., Franssen, J.M.. Numerical analysis of stainless steel beam-columns in case of fire. Fire Safety Journal 2012;50:35–50.
[62] Selamet, S., Garlock, M.E.. Plate buckling strength of steel wide-flange sections at elevated temperatures. Journal of Structural Engineering, ASCE 2013;139(11):1853–1865.
[63] Couto, C., Vila Real, P., Lopes, N., Zhao, B.. Resistance of steel cross-sections with local buckling at elevated temperatures. Journal of Constructional Steel Research 2015;109:101–114.
[64] Couto, C., Vila Real, P., Lopes, N., Zhao, B.. Numerical investigation of the lateral–torsional buckling of beams with slender cross sections for the case of fire. Engineering Structures 2016;106:410–421.
[65] Varol, H., Cashell, K.. Numerical modelling of high strength steel beams at elevated temperature. Fire Safety Journal 2017;89:41–50.
[66] Possidente, L., Tondini, N., Battini, J.M.. Torsional and flexural-torsional buckling of compressed steel members in fire. Journal of Constructional Steel Research 2020;171:106130.
[67] Martins, A.D., Gonçalves, R., Camotim, D.. Numerical simulation and design of stainless steel columns under fire conditions. Engineering Structures 2021;229:111628.
[68] Martins, A.D., Camotim, D., Gonçalves, R., Lopes, N., Vila Real, P.. Transversally loaded stainless steel beams under fire: Local/global behaviour, strength and design. Journal of Constructional Steel Research 2022;189:107080.
[69] ISO 834-1. Fire-resistance tests — Elements of building construction - Part 1: General requirements. International Organization for Standardization (ISO), Geneva; 1999.
[70] Gardner, L., Ng, K.. Temperature development in structural stainless steel sections exposed to fire. Fire Safety Journal 2006;41(3):185–203.
[71] Kruppa, J.. Eurocodes–Fire parts: Proposal for a methodology to check the accuracy of assessment methods. CEN TC 250, Horizontal Group Fire, Document no: 99/130; 1999.